Supporting information

Metabolic Engineering-Based Rapid Characterization of a Sesquiterpene Cyclase and the Skeletons of Fusariumdiene and Fusagramineol from *Fusarium graminearum*

Guangkai Bian[†#], Anwei Hou[†#], Yujie Yuan[†], Ben Hu[†], Shu Cheng[†], Ziling Ye[‡], Yingtong Di[§|], Zixin Deng[†,||], Tiangang Liu[†,||*]

[†]Key Laboratory of Combinatorial Biosynthesis and Drug Discovery, Ministry of Education and School of Pharmaceutical Sciences, Wuhan University, Wuhan 430071, P. R. China.

[‡]J1 Biotech Co., Ltd., Wuhan 430075, P. R. China.

[§]State Key Laboratory of Phytochemistry and Plant Resources in West China, Kunming Institute of Botany, Chinese Academy of Sciences, Kunming 650204, P. R. China.

[||]Hubei Engineering Laboratory for Synthetic Microbiology, Wuhan Institute of Biotechnology, Wuhan 430075, P. R. China

Table of Contents

Supplementary Materials and Methods

Strains and media

E. coli BL21 (DE3) *F⁻dcm ompT hsdSB(rB⁻mB⁻)gal* was obtained from Invitrogen (Carlsbad, CA, USA). *S. cerevisiae* CEN.PK2-1D (European *Saccharomyces cerevisiae* archive for functional analysis [EUROSCARF] accession number: 30000B) was purchased from EUROSCARF (Oberuresel, Germany) and cultivated in YPD medium. *F. graminearum* J1-012 was isolated from *Taxus chinensis* and cultivated in PDA medium. Whole genome sequencing and analysis of *F. graminearum* J1-012 is described in our previous work.[1]

Phylogenetic analysis of terpene synthases of genus *Fusarium* and *F. graminearum* J1-012

For genus *Fusarium*, multiple sequence alignment was performed using Muscle. Evolutionary analyses were conducted in MEGA7.[2] A phylogenetic tree was inferred using the maximum likelihood method based on the Jones-Taylor-Thornton (JTT) matrix-based model. This analysis involved seventy-eight amino acid sequences. All positions with less than 95% site coverage were eliminated. There were a total of 138 positions in the final dataset.

Construction of plasmids and mutants

The primers used in this study are listed in Table S1. Strains and plasmids are summarized in Table S2. To construct the plasmid to express sufficient precursor IPP and DMAPP in *S. cerevisiae*, pZY141 was constructed according to the following procedure: the left and right homologous arms of *GAL1710* and the terminator *CPS1* were amplified from *S. cerevisiae* CENPK2-1D using the primer pairs P1/P2, P3/P4, and P5/P6, respectively; *TRP1* was amplified from pRS424 using primer pair P7/P8; *ACT1* and *tHMG1* were amplified from *S. cerevisiae* S288C using primer pairs P9/P10 and P11/P12,

respectively; the promoter *PGAL10-PGAL1* and the plasmid backbone were amplified from *S. cerevisiae* CENPK2-1D and pRS426 using primer pairs P13/P14 and P15/P16, respectively. Then, *TRP1*, *ACT1*, and the left homologous arm of *GAL1710* were assembled using splicing by overlap extension PCR (SOE-PCR)[3] using the primer pair P1/P10; *tHMG1*, *PGAL10-PGAL1*, and *CPS1* were assembled by the same method using the primer pair P11/P6. Finally, the assembled fragments, together with the amplified backbone of pRS426 and the right homologous arm of *GAL1710*, were assembled using the yeast assembly method to generate the final plasmid pZY141.

To overexpress FgFS in *E. coli*, the coding sequence of *FgJ03939* was amplified from the cDNA library of *F. graminearum* using primer pair P17/P18, and then the fragment was subcloned into pET28a to generate pGB152. To verify the function of FgFS in *S. cerevisiae*, pGB315 was constructed according to the following procedure: *FgJ03939* was amplified from pGB152 using primer pair P19/P20; *ERG20* was amplified from *S. cerevisiae* CENPK2-1D using primer pair P21/P22; *PGAL1-GAL10* was amplified from pZY141 using primer pair P23/P24; and the plasmid backbone was amplified from pXL144 (constructed by Xiaowei Li, unpublished data) using primer pair P25/P26. Finally, the above amplified fragments were assembled using the Gibson method to generate pGB315.[4]

Plasmid pZY141 was linearized and inserted into the *GAL1710* site of *S. cerevisiae* CENPK2-1D to generate the mutant *S. cerevisiae* ZY141. Thereafter, pGB315 with the downstream sesquiterpene-forming pathway was linearized and inserted into the HIS3 site of *S. cerevisiae* ZY141 to generate *S. cerevisiae* T16.

Protein expression and purification

Plasmid pGB315 was transformed into *E. coli* BL21 (DE3) and cultivated in 2-L flasks containing 1 L LB medium at 37 ℃ with 50 mg/L kanamycin (KAN). When the OD_{600} reached 0.6–0.8, 0.1 mM IPTG was added to the cultures, which were then cultivated for an additional 6 h at 28 ℃. The cells were harvested and resuspended in 40 mL buffer A

(50 mM Tris-Cl, 300 mM NaCl, 4 mM β-mercaptoethanol, pH 7.6). Cell disruption was performed using a high-pressure homogenizer and centrifuged at 30,000 × *g* for 1 h. A Biologic DuoFlow Chromatography System (Bio-Rad Laboratories, Hercules, CA, USA) was used for protein purification. His-tagged proteins were purified by Ni-NTA affinity chromatography (GE Healthcare, Little Chalfont, UK), anion exchange resin (HiTrap Q FF; GE Healthcare), and gel filtration chromatography (HiPrep 16/60 Sephacryl S-200 HR; GE Healthcare). The purified protein (Figure S4) was then concentrated and preserved in 50 mM Tris buffer (50 mM Tris, 10% glycerol). The protein concentration was measured using a Pierce1 BCA protein assay kit (Thermo Fisher Scientific, Waltham, MA, USA) and recorded on an Enspire Multimode Plate Reader (PerkinElmer, Waltham, MA, USA).

***In vitro* assays and kinetic measurements**

To test the terpene synthase activity of FgFS, an *in vitro* assay was carried out as previously described.[1] Reactions were carried out using 10 μM FgFS, 100 μM substrates (GPP, FPP, or GGPP), and 2 mM Mg^{2+} in 200 μL 50 mM Tris-HCl buffer (pH 7.6) with 10% glycerol at 30 ℃ overnight. The products were extracted with an equal volume of hexane and then detected and analyzed by GC/MS (Figure S6, S7). For steady-state kinetics, 100-μL scale reactions were carried out in 50 mM Tris-HCl buffer (pH 7.6) with 10% glycerol and 50 μL pyrophosphate reagent. Reactions were carried out with 1 mg/mL FgFS, 2 mM Mg^{2+}, and 1–200 mM substrates (GPP, FPP, and GGPP). Product assays were carried out by measuring the release of pyrophosphate (PPi), which was recorded using an Enspire Multimode Plate Reader, as previously described (Table S3).[5]

Expression and functional characterization of FgFS in *S. cerevisiae*

S. cerevisiae T16 was cultivated in YPD media in a shake flask and then inoculated into a 5-L fermenter with 2.5 L YPD at 30 ℃. A two-stage feeding process was adopted in this fed-batch fermentation. First, 1.5-L feeding solution with 10 g/L yeast extract and 500 g/L glucose was used to sustain rapid cell growth. When the cells reached the stable

phase, 1% galactose was added to the fermenter to induce the production of sesquiterpenes. Ethanol (feeding solution II) was used as carbon source to meet the needs of cell metabolism. The isotopic labeling experiment was carried out in a 5-L fermenter with 2 L YPD. Feeding solution II was replaced with 50 g/L glucose, 450 g/L sodium acetate, and 1% [1-^{13}C,2-$^{2}H_3$] - sodium acetate. The pH was controlled at 6.0 to maintain an acidic environment for normal metabolism. Cell growth and the accumulation of sesquiterpenes were monitored through the fermentation process.

Compound isolation and structure elucidation

The sesquiterpenes were isolated from the hexane-extracted layer of the fermentation broth and cells of *S. cerevisiae* T16 (200 mL) using XBridge^{TM} Prep C18 column (Waters, 10 × 250 mm, 5 μm) and prep-HPLC system with acetonitrile and water as the mobile phase. The first round isolation was carried out according to the following procedure: flow rate, 2.5 mL/min; in the first 85 min, the proportion of acetonitrile was increased using a linear gradient from 20% to 90%; the proportion of acetonitrile was then increased to 100% over 1 min and maintained for 10 min; finally, the proportion of acetonitrile was decreased to 20% and maintained for 10 min. Compound **1** was isolated with a retention time of 95.2 min (5.6 mg). Compound **4** was isolated with a retention time of 72.4 min (14.2 mg). Compound **6** was isolated with a retention time of 92.4 min (1.5 mg). Compound **8** was isolated with a retention time of 95.2 min (2.3 mg). Compound **2**, **3**, **5** and **7** were located in the F1 to F4 fractions with retention times of 61.3–64.8 min, 65.5–67.3 min, 70.4–72.0 min and 69.9–70.9 min, respectively. Thereafter, compound **2** (25.7 mg), with a retention time of 46.8 min, was isolated from F1 using 75% acetonitrile as the mobile phase at a rate of 0.75 mL/min. Compound **3** (40.3 mg), with a retention time of 25.7 min, was isolated from F2 using 70% acetonitrile as the mobile phase at a rate of 2 mL/min. Compound **5** (11.3 mg), with a retention time of 36.5 min, was isolated from F3 using 92% acetonitrile as the mobile phase at a rate of 0.6 mL/min. Compound **7** (2.1 mg), with a retention time of 33.2 min, was isolated from

F4 using 96% acetonitrile as the mobile phase at a rate of 0.6 mL/min. ^{1}H NMR and ^{13}C NMR were performed on an Agilent 400 MHz or 600 MHz instrument (DirectDrive2; Santa Clara, CA, USA).

Compound **1**. Colorless oil. $[\alpha]_D^{22}$ = -13.8 (*c* 0.4, $CHCl_3$). For NMR data, see Table S4 and Figure S8. HRMS (ESI) calculated for $C_{15}H_{23}$ $[M-H]^+$: m/z 203.1794; m/z found: 203.1792.

Compound **2**. White solid. $[\alpha]_D^{22}$ = -45.6 (*c* 0.26, $CHCl_3$). For NMR data see Table S5 and Figure S9. HRMS (ESI) calculated for $C_{15}H_{25}$ $[M-OH]^+$: m/z 205.1951; m/z found: 205.1950.

Compound **3**. White solid. $[\alpha]_D^{22}$ = -72.3 (*c* 0.25, $CHCl_3$). For NMR data see Tables S6 and Figure S10. HRMS (ESI) calculated for $C_{15}H_{25}$ $[M-OH]^+$: m/z 205.1951; m/z found: 205.1951.

Compound **4** was identified as nerolidol. Colorless oil. $[\alpha]_D^{22}$ = 20.1 (*c* 0.04, benzene). ^{1}H NMR (400 MHz, $CDCl_3$) δ [ppm] = 5.92 (dd, *J* = 17.3, 10.8 Hz, 1H), 5.21 (dd, *J* = 17.3, 1.3 Hz, 1H), 5.14 (tt, *J* = 5.8, 1.3 Hz, 1H), 5.11 – 5.06 (m, 1H), 5.06 (dd, *J* = 10.8, 1.3 Hz, 1H), 2.11 – 2.01 (m, 4H), 2.00 – 1.96 (m, 2H), 1.68 (s, 3H), 1.60 (d, *J* = 1.2 Hz, 6H), 1.60 (d, *J* = 9.5 Hz, 2H), 1.28 (s, 3H) (Figure S11a). ^{13}C NMR (101 MHz, $CDCl_3$) δ [ppm] = 145.0, 135.5, 131.4, 124.1, 124.1, 111.6, 73.5, 41.9, 39.6, 27.8, 26.6, 25.6, 22.6, 17.6, 15.9 (Figure S11b). HRMS (ESI) calculated for $C_{15}H_{25}$ [M-OH]+: m/z 205.1951; m/z found: 205.1940. These data were the same as previously reported.[1, 6]

Compound **5** was identified as (-)-α-acorenol. Colorless oil. $[\alpha]_D^{22}$ = -30.7 (*c* 0.07, $CHCl_3$). ^{1}H NMR (400 MHz, $CDCl_3$) δ [ppm] = 5.45 – 5.39 (m, 1H), 2.40 – 2.30 (m, 1H), 2.03 – 1.90 (m, 3H), 1.89 – 1.85 (m, 2H), 1.85 – 1.80 (m, 1H), 1.80 – 1.70 (m, 1H), 1.67 – 1.64 (m, 3H), 1.55 – 1.45 (m, 2H), 1.43 – 1.35 (m, 1H), 1.26 – 1.24 (m, 1H), 1.21 (s, 3H), 1.21 (s, 3H), 0.85 (d, *J* = 6.8 Hz, 3H) (Figure S12a). ^{13}C NMR (101 MHz, $CDCl_3$) δ [ppm] = 135.2, 121.2, 73.7, 54.7, 45.0, 41.7, 31.5, 30.6, 30.1, 29.0, 27.9, 27.8, 26.1, 23.3,

14.9 (Figure S12b). HRMS (ESI) calculated for $C_{15}H_{25}O$ $[M]^+$: m/z 221.1900; m/z found: 221.1897. These data were the same as previously reported.[7]

Compound **6** was identified as (*E*)-β-farnesene. Colorless oil. ^{1}H NMR (400 MHz, $CDCl_3$) δ [ppm] = 6.3 (dd, *J* = 17.6, 10.8 Hz, 1H), 5.2 (dd, *J* = 17.6, 1.1 Hz, 1H), 5.1 – 5.0 (m, 2H), 5.0 – 4.9 (m, 3H), 2.2 – 2.1 (m, 3H), 2.1 – 1.9 (m, 5H), 1.6 (d, *J* = 1.5 Hz, 3H), 1.6 (d, *J* = 1.5 Hz, 6H) (Figure S13a). ^{13}C NMR (101 MHz, $CDCl_3$) δ [ppm] = 146.0, 138.9, 135.3, 131.3, 124.3, 123.9, 115.7, 113.0, 39.6, 31.3, 26.6, 26.5, 25.7, 17.6, 16.0 (Figure S13b). HRMS (ESI) calculated for $C_{15}H_{24}$ $[M]^+$: m/z 204.1873; m/z found: 204.1869. These data were the same as previously reported.[8]

Compound **7** was identified as (+)-α-bisabolol. Colorless oil. $[\alpha]_D^{22}$ = 51.3 (*c* 0.06, $CHCl_3$). ^{13}C NMR (101 MHz, $CDCl_3$) δ [ppm] = 134.1, 131.7, 124.4, 120.4, 74.2, 42.8, 40.0, 30.9, 26.8, 25.6, 23.3, 23.2, 23.1, 21.9, 17.6 (Figure S14). HRMS (ESI) calculated for $C_{15}H_{25}O$ $[M]^+$: m/z 221.1900; m/z found: 221.1898. These data were the same as those previously reported findings.[9]

Compound **8** was identified as (-)-acoradiene.[10] Colorless oil. $[\alpha]_D^{22}$ = -24.2 (*c* 0.06, $CHCl_3$). The molecular formula was determined as $C_{15}H_{26}O$ by HR-ESI-MS at *m/z* 204.1873 $[M]^+$ (calcd 204.1873). Our ^{1}H-NMR data revealed the existence of one singlet methyl (Me-12), three doublet methyls (Me-13, Me-14 and Me-15), and two olefinic methines (H-2, H-9) (Table S7 and Figure S15b). The ^{13}C-NMR and HSQC spectra confirmed the presence of fifteen carbon atoms, which were assigned as one sp^3 quaternary carbon (C-6), two sp^2 quaternary carbons (C-3, C-10), two olefinic methines, two aliphatic methines, four aliphatic methylenes, and four methyls. These data designated the bicyclic skeleton for compound **8**. Our ^{1}H-^{1}H COSY experiments then revealed spin systems of H-1/H-2, H-4/H-5, H-13/H-7/H-8/H-9, and H-14/H-11/H-15 (Figure S15a and 15e). Additionally, HMBC from the methyl signals were observed as follows: Me-12 to C-2, C-3, and C-4; Me-13 to C-6, C-7, and C-8; Me-14 to C-10, C-11, and C-15; and M-15 to C-10, C-11, and C-14. Furthermore, the HMBC spectra showed

correlations between H-5 and C-1, C-6 and C-7, between H-9 and C-6 and C-7, and between H-11 and C-9 (Figure S15a and 15f). Thus, the planar structure of compound **8** was identified as a 5/6-membered spirocyclic sesquiterpene.

Calculation of optical rotation

All quantum-chemical calculations were performed using the Gaussian 03 program. The optical rotation calculations were calculated using the b3lyp/aug-cc-pvdz method under the Self-Consistent Reaction Field model of solvent ($CHCl_3$).

Energy minimization and optical rotation calculations

The initial conformational distribution search was performed using the MMFF94 method overlaid with key correlations observed in the NOESY spectra of **1**. The corresponding minimum geometries were preoptimized at the HF/6-31G level in Gaussian 03 program package,[11] which was further checked by frequency calculations; no imaginary frequencies were found. Their minimum geometries were further optimized by DFT calculation B3LYP at the b3lyp/aug-cc-pvdz level in the gas phase. ECD calculations were performed on the obtained stable conformers by TDDFT [b3lyp/aug-cc-pvdz] under the Self-Consistent Reaction Field model of solvent ($CHCl_3$). The overall predicted specific rotation value of **1** was subsequently compared with that of the experimental one.

The cDNA sequence of FgFS:

ATGCCTCACAAGCACGTTCCTCTTAGACCAGTCAAGTTGACATTTGATCCTGTAGGATCA
AACACCCTAGGTGTGCCAACCTTGGACTTTGAGTCTCTGTTCCGGGAAGACAGCGTCTCT
GAGGATGCCCCTCTTGTTATCTACCCAGAGGATATGGGTGTCCCATGGAACACCTCTCTT
CCTTGGACCAGACAATCCAAGTTCTGGGCTTACGCCGAGGCAGCTGGATATGAAATGGCC
AACGGAATCAGCCTTGACAAGGCATCAGAGCGTGGCACACTACCCATGGAGTTGATGGA
TGAGCGTCGCAAGTGGAAGATTGATGAGCTAGTTGAGGATGCCATCTCTTGCTGTGCTTA
TCTTTACCCTACATCATCTCCTACCAGATTGGCGTTGTTGACCCAGTCTGTTCTGCTTCTAT

TCCTCCACGACGATGTTATTGAGCGAGGAGCTACTCAAAACGAAACCACAGTGGTAGAC

GAATTTCTTAGCATGGCTCCCAAGAACAGGCATCTTAAGAAATTCTGGTCAGACGTATTG

GAATGTGATCCCGTCCTTGGACCTGATCTGCTTTATGCTATCCATGCTTTCGTCCGTGATG

GTCGTGTAAAGTCACCCTTTAAGCAGGATCACTATGCCACATTGGCTGATTACATGCTTT

ACCGTCGCAATGATGTTGGCAAGACATTTATGATTGCAGCTATCCGCTTCGGCTCTGGCG

TGCAACAAACACGCGAAGAACTTGCTCCCTTTGACGAGCTTGCTGATCTTTACGTCAGAC

ACTCAATTCTTATCAACGATCTCTACTCGTATGATAAGGAGGTGCACGAGGTCAAGACTA

TCGACGCGTCCATCGTGAACGCAGTTGCTGTCACAGAGCAGCTCCTTTCCGTGTCGCCTG

ACCTGGCCAAGAACTTAACCAGAGCTATTACCTTTGACATGGAGAAGGAGTTTTACGGCA

TTTGTGAGAAGTTTATGCACAGCCCTGATATCAACGATCGCCAGCGCGTGTTCGTTACTG

CGCTCTTTGATGCGTTGACAGGCAATATCTTCCATTCTGCTACTTTGAGCAGATACGTTCG

TCACGGCGAGAGACCACTTCCTTGCAAGTGTTAG

References:

(1) Bian, G.; Han, Y.; Hou, A.; Yuan, Y.; Liu, X.; Deng, Z.; Liu, T. *Metab. Eng.* **2017,** *42*, 1-8.

(2) Kumar, S.; Stecher, G.; Tamura, K. *Mol. Biol. Evol.* **2016,** *33* (7), 1870-1874.

(3) Shevchuk, N. A.; Bryksin, A. V.; Nusinovich, Y. A.; Cabello, F. C.; Sutherland, M.; Ladisch, S. *Nucleic Acids Res.* **2004,** *32* (2), e19.

(4) Gibson, D. G.; Young, L.; Chuang, R. Y.; Venter, J. C.; Hutchison, C. A.; Smith, H. O. *Nat. Methods* **2009,** *6* (5), 343-345.

(5) Agger, S. A.; Lopez-Gallego, F.; Hoye, T. R.; Schmidt-Dannert, C. *J. Bacteriol.* **2008,** *190* (18), 6084-6096.

(6) Doskotch, R.; Cheng, H.-Y.; Odell, T.; Girard, L. *J. Chem. Ecol.* **1980,** *6* (4), 845-851.

(7) Brock, N. L.; Huss, K.; Tudzynski, B.; Dickschat, J. S. *Chembiochem.* **2013,** *14* (3), 311-5.

(8) Simionatto, E.; Porto, C.; Stüker, C. Z.; Dalcol, I. I.; Silva, U. F. d. *Quim. Nova* **2007,** *30* (8), 1923-1925.

(9) (a) Miyazawa, M.; Nankai, H.; Kameoka, H. *Phytochemistry* **1995,** *39* (5), 1077-1080; (b) Günther, K.; Carle, R.; Fleischhauer, I.; Merget, S. *Fresenius J. Anal. Chem.* **1993,** *345* (12), 787-790.

(10) Marx, J. N.; Norman, L. R. *J. Org. Chem.* **1975,** *40* (11), 1602-1606.

(11) Frisch, M.; Trucks, G.; Schlegel, H.; Scuseria, G.; Robb, M.; Cheeseman, J.; Montgomery Jr, J.; Vreven, T.; Kudin, K.; Burant, J., gaussian 03, Gaussian. *Inc.: Wallingford, CT* **2004**.

247

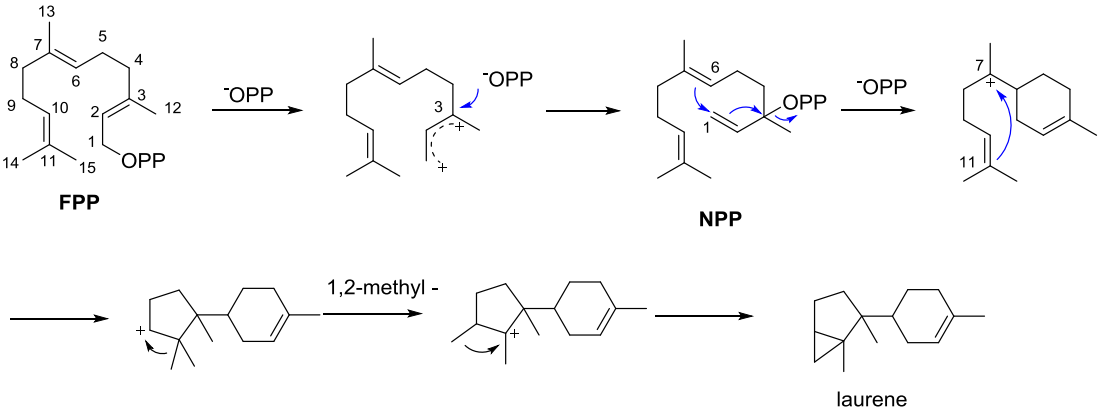

248

249 **Figure S1.** The skeleton produced by 1,6-cyclization of FPP upon isomerization to

250 nerolidyl pyrophosphate (NPP).

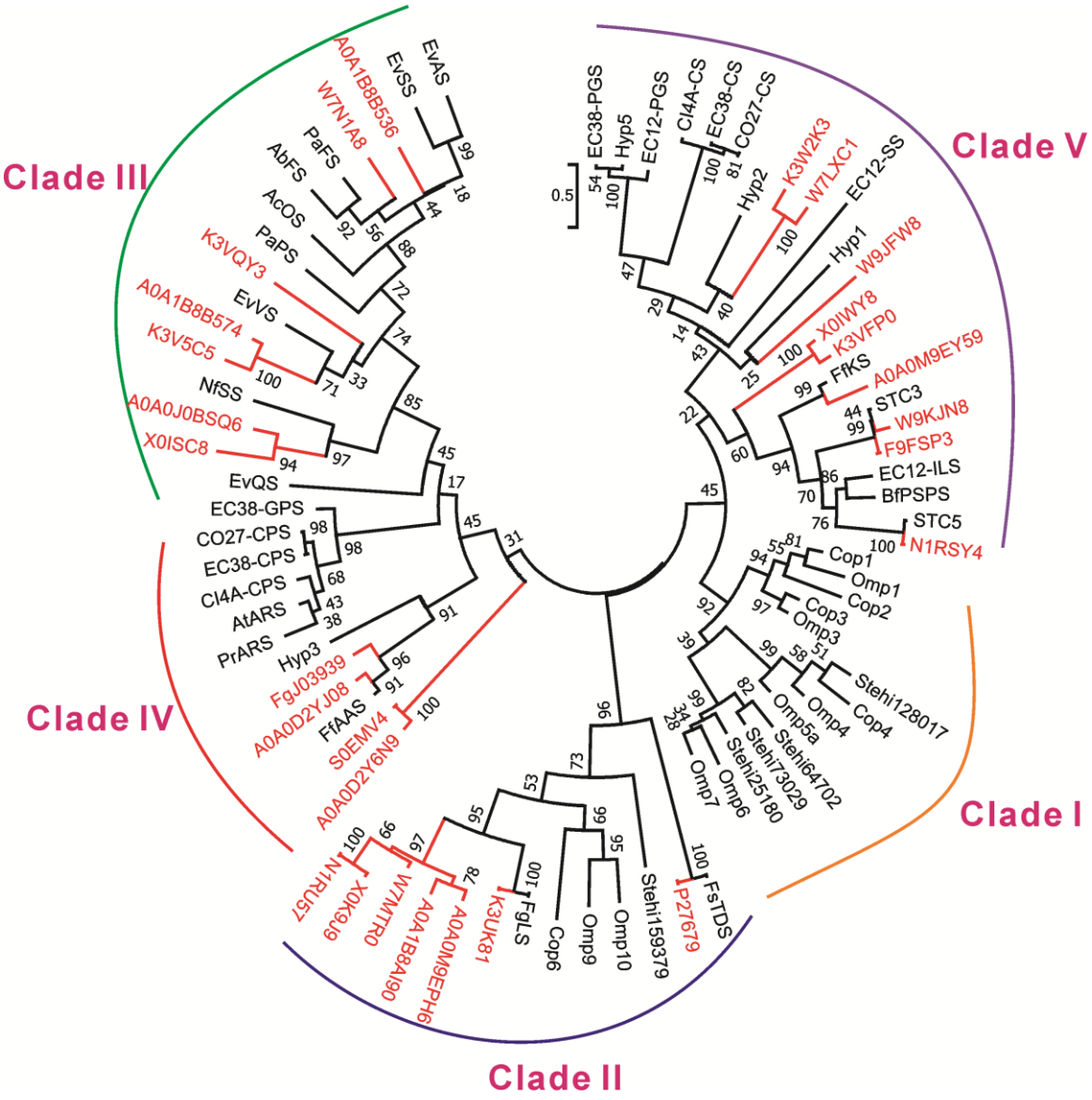

Figure S2. Phylogenetic tree of class I terpene synthases in genus *Fusarium*. Branches marked in red represent the terpene synthases from genus *Fusarium*. Branches for identified terpene synthases of filamentous fungi are marked in black. Branch length indicates the number of substitutions per site. Branches are labeled with the percentage base on 1, 000 bootstrap replicates.

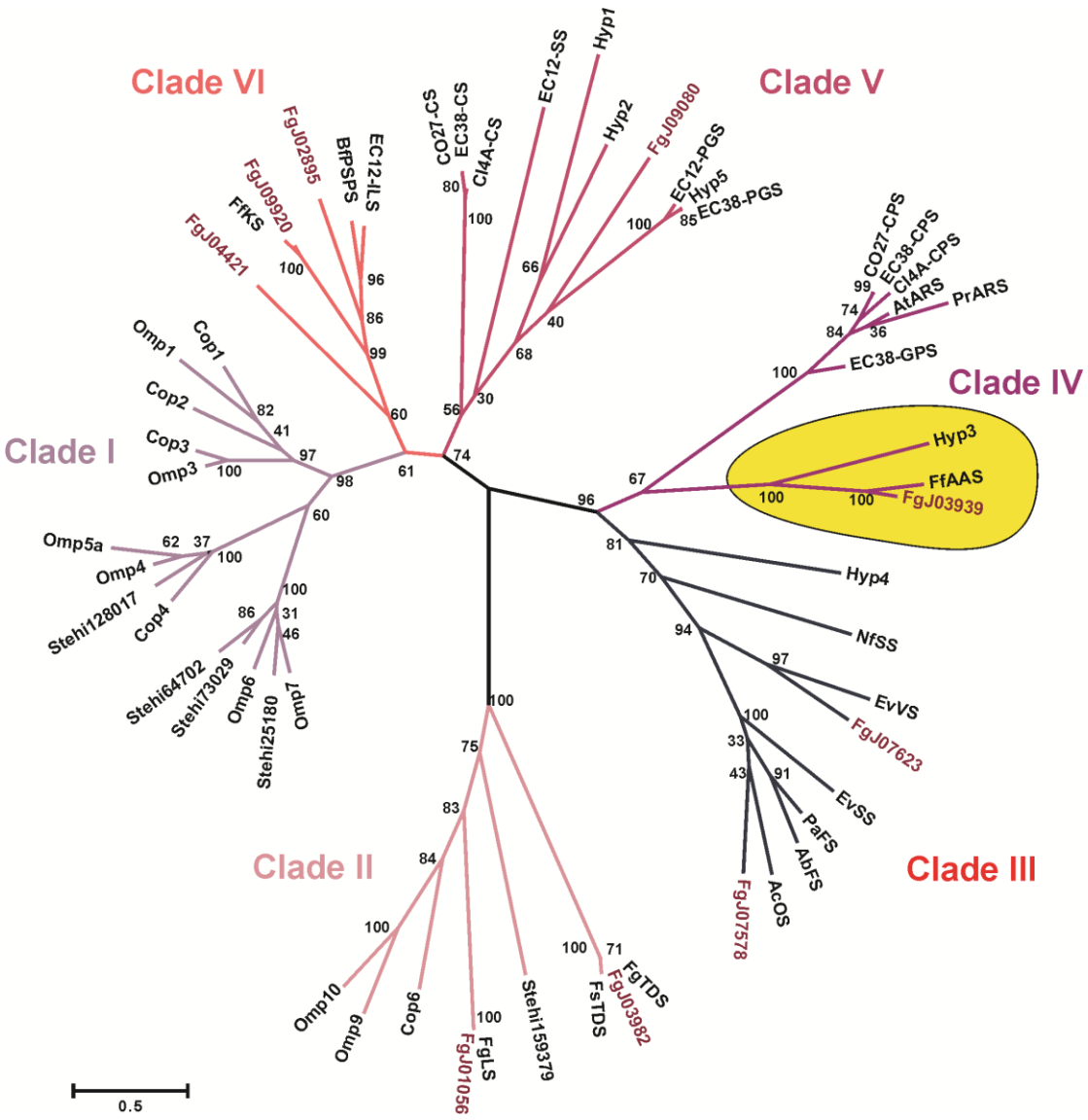

Figure S3. Phylogenetic tree of class I terpene synthases in *F. graminearum* J1-012. Nine terpene synthases of *F. graminearum* J1-012 are designated as FgJ0xxxx and marked in red. Branches of identified terpene synthases of filamentous fungi are marked in black. Branch length indicates the number of substitutions per site. Branches are labeled with the percentage based on 1,000 bootstrap replicates.

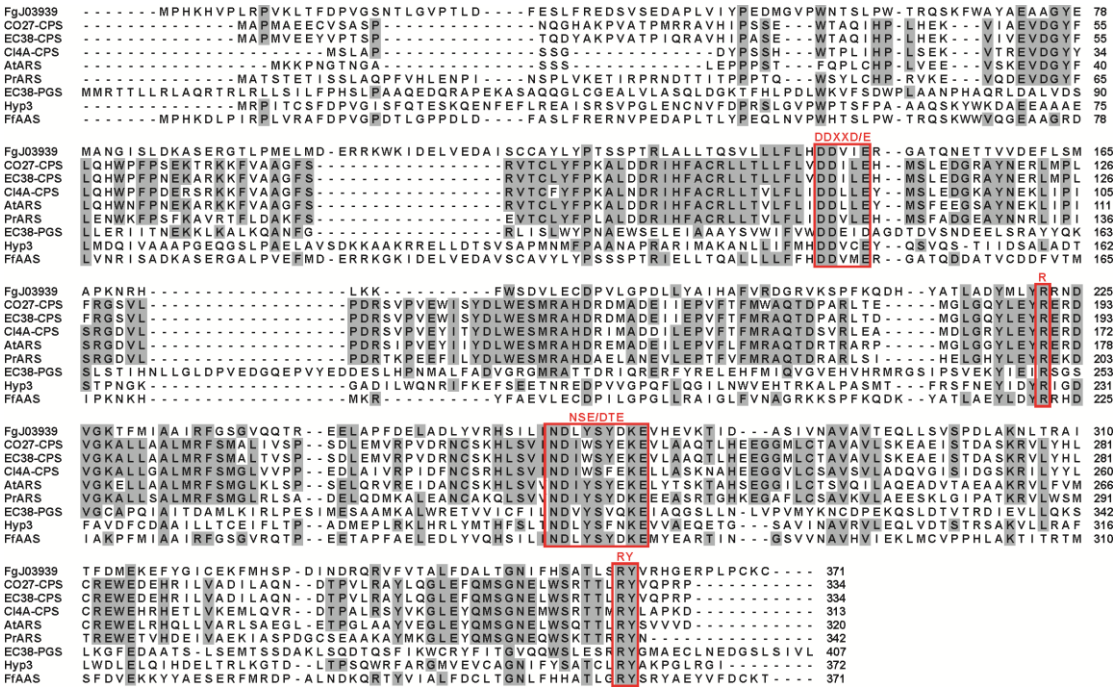

Figure S4. Sequence alignment of FgFS and the clade IV of fungi class I terpene synthase. The red boxes represent the conserved "DDXXD/E", "NSE/DTE", "R", and "RY" motifs.

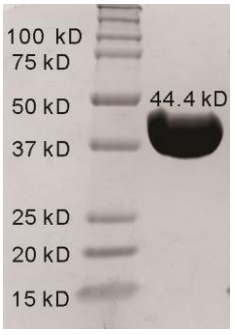

Figure S5. SDS-PAGE analysis of recombinant sesquiterpene cyclase FgJ03939.

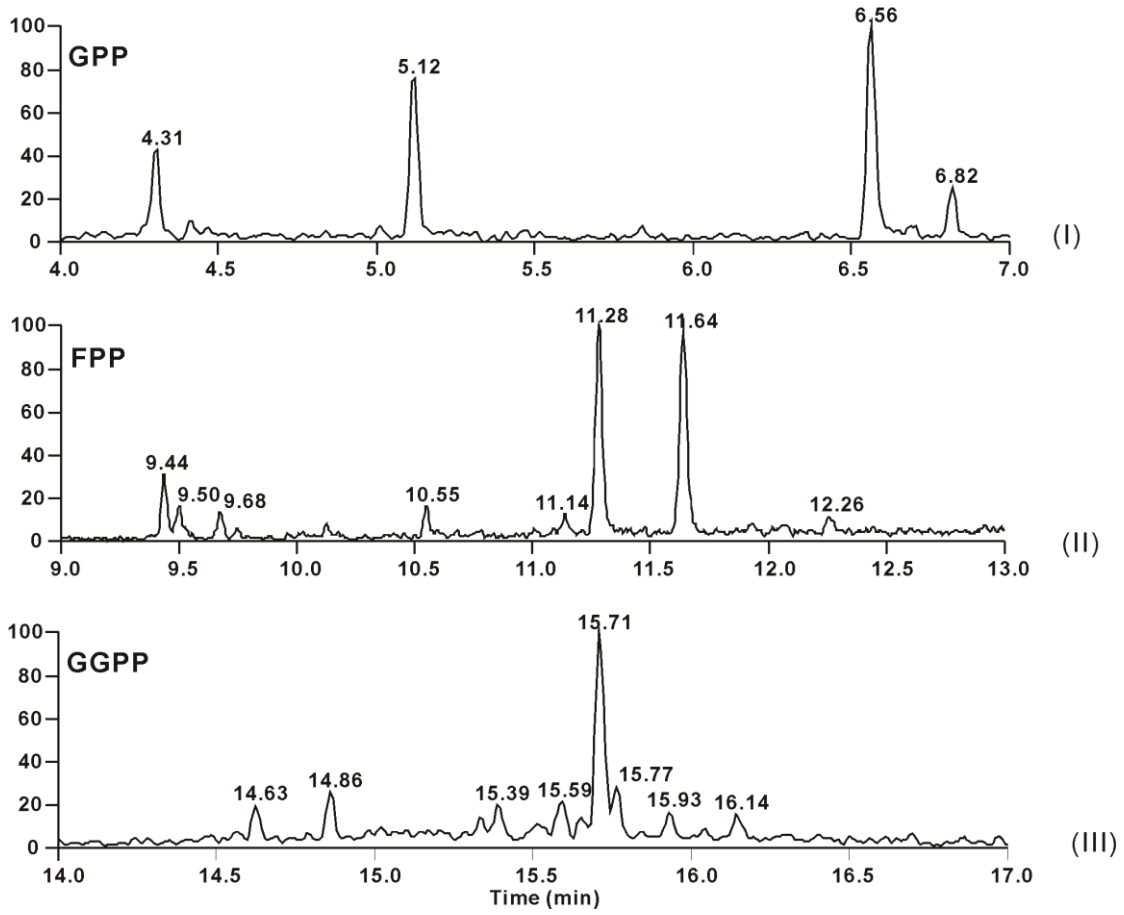

Figure S6. *In vitro* assay of purified FgFS by using GPP (i), FPP (ii), and GGPP (iii) as substrate, respectively.

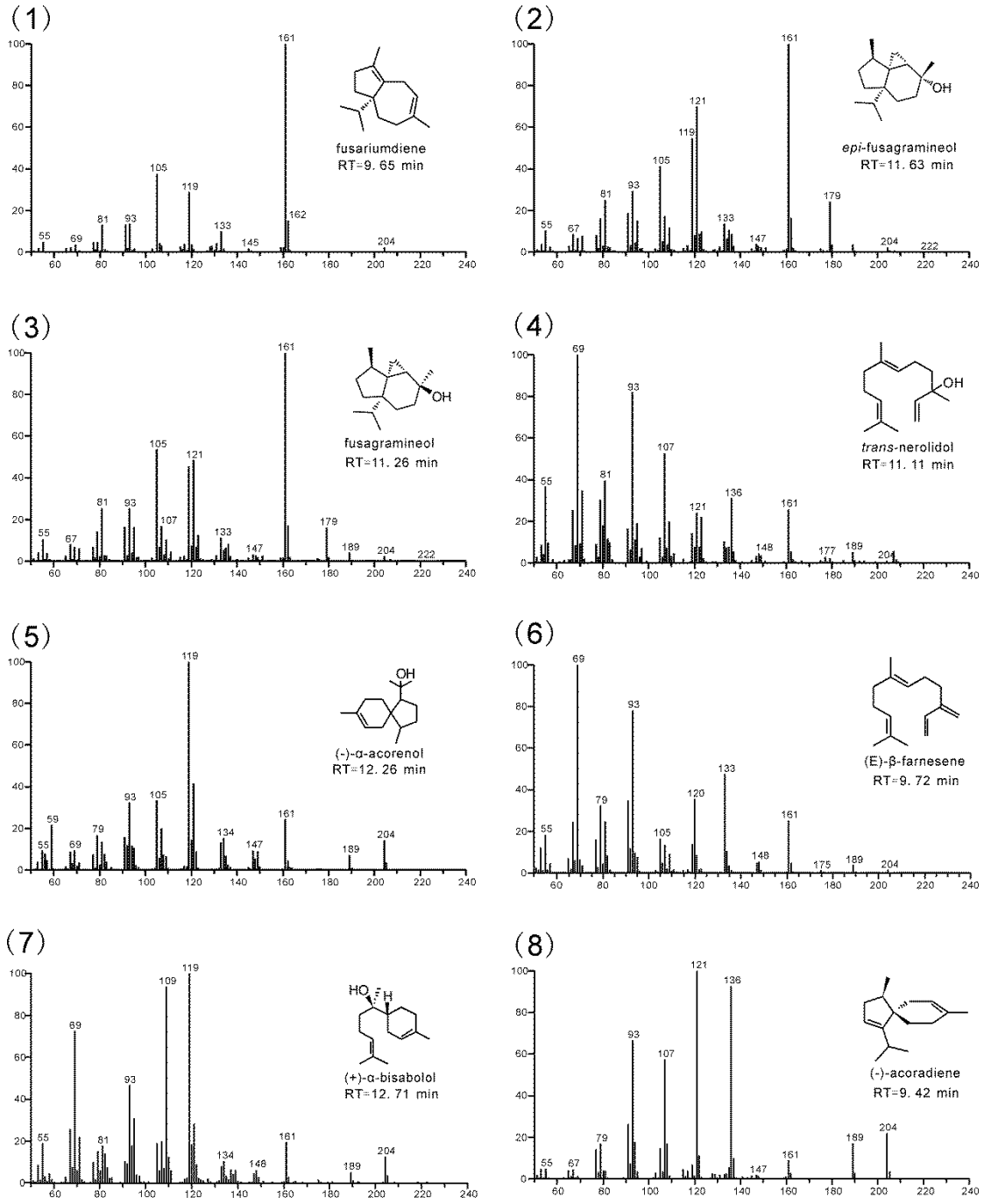

Figure S7. Mass spectra of sesquiterpenes produced by FgFS.

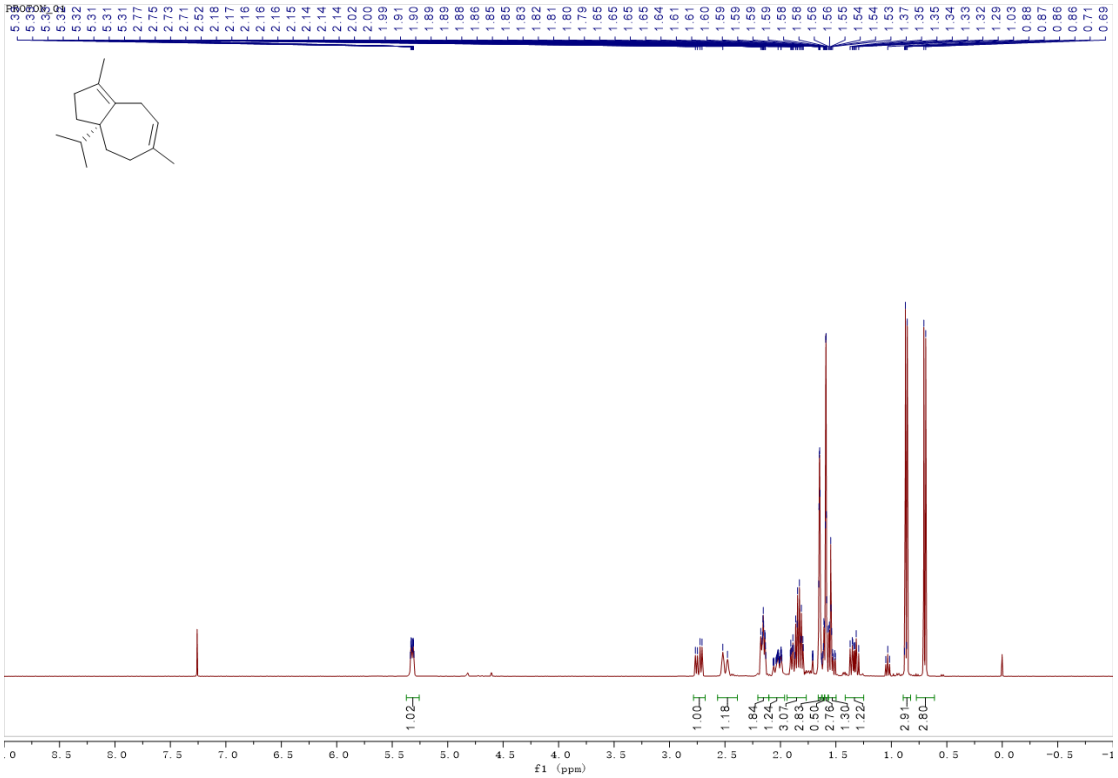

Figure S8a. ^{1}H NMR spectrum of compound **1** ($CDCl_3$, 400 MHz).

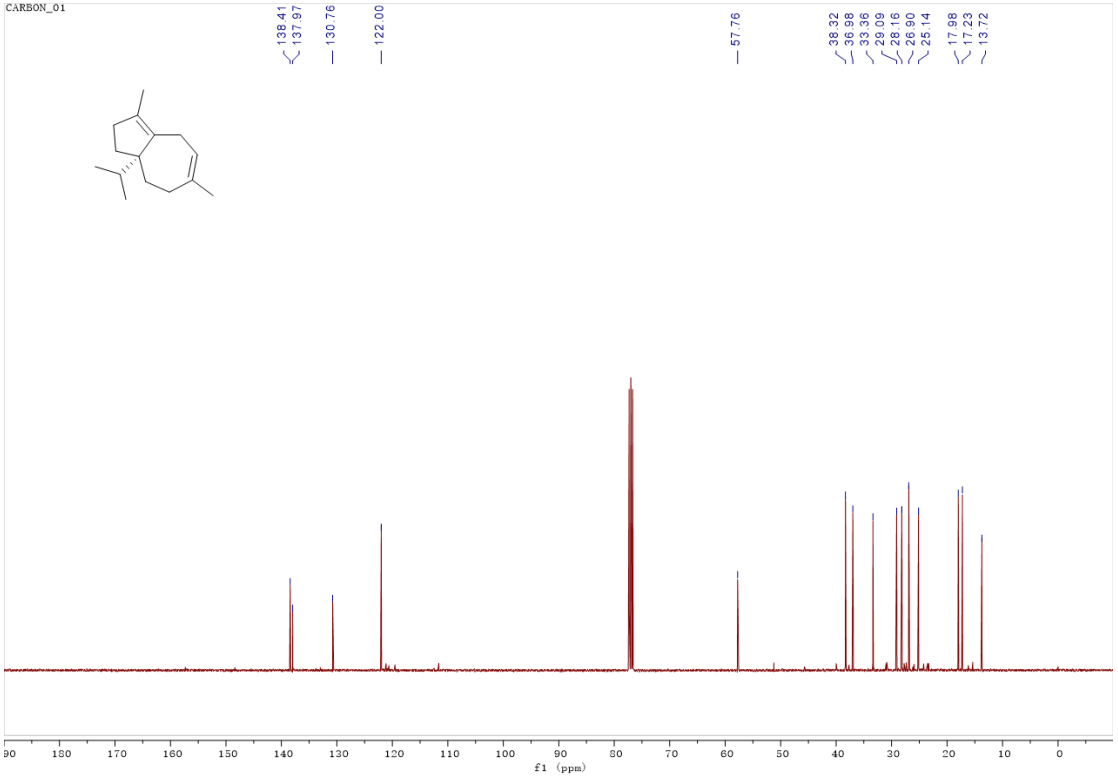

Figure S8b. ^{13}C NMR spectrum of compound **1** ($CDCl_3$, 101 MHz).

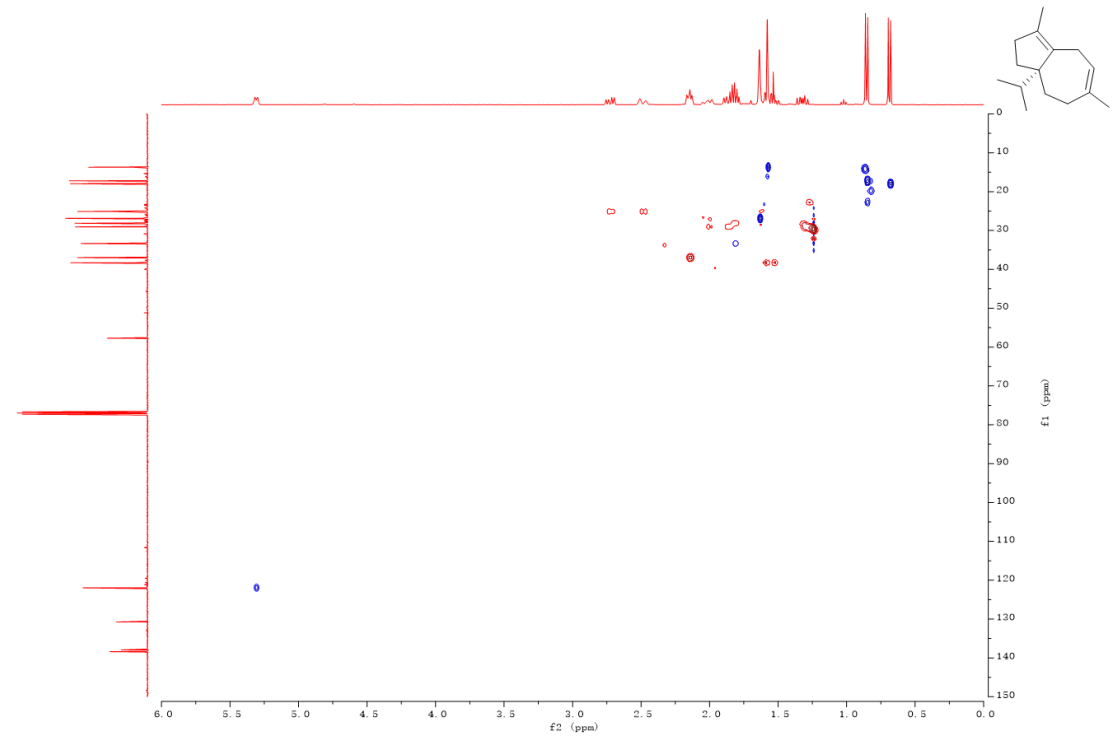

Figure S8c. HSQC spectrum of compound **1** in $CDCl_3$.

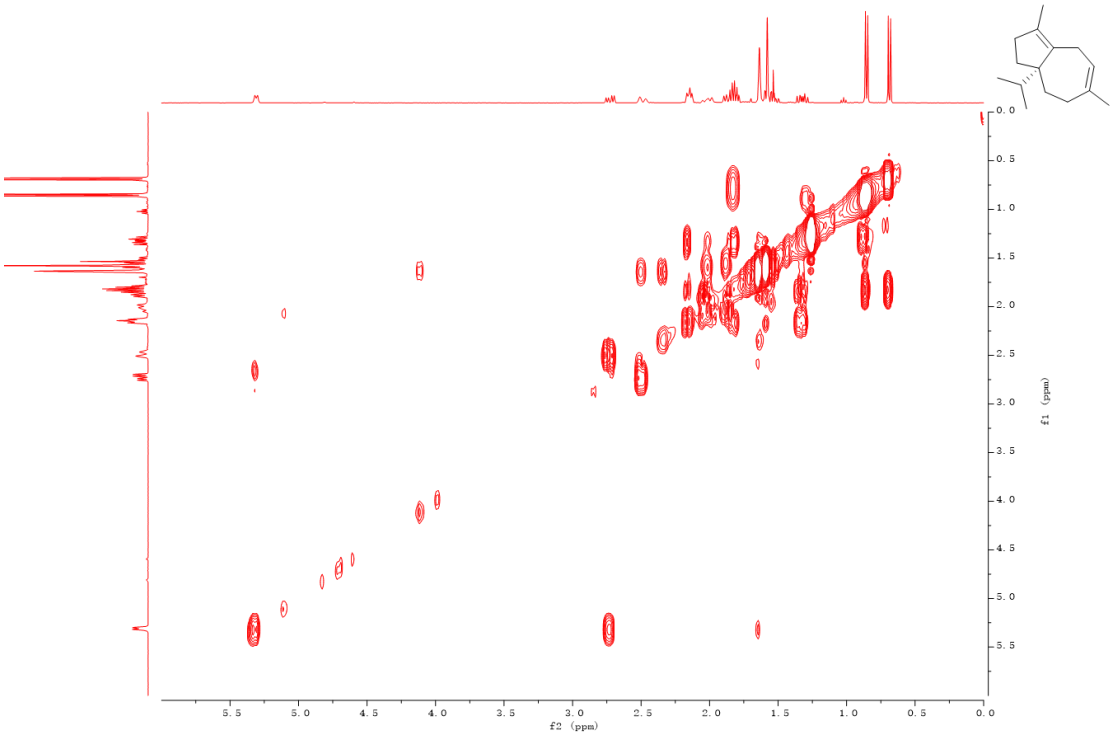

Figure S8d. ^{1}H-^{1}H COSY spectrum of compound **1** in $CDCl_3$.

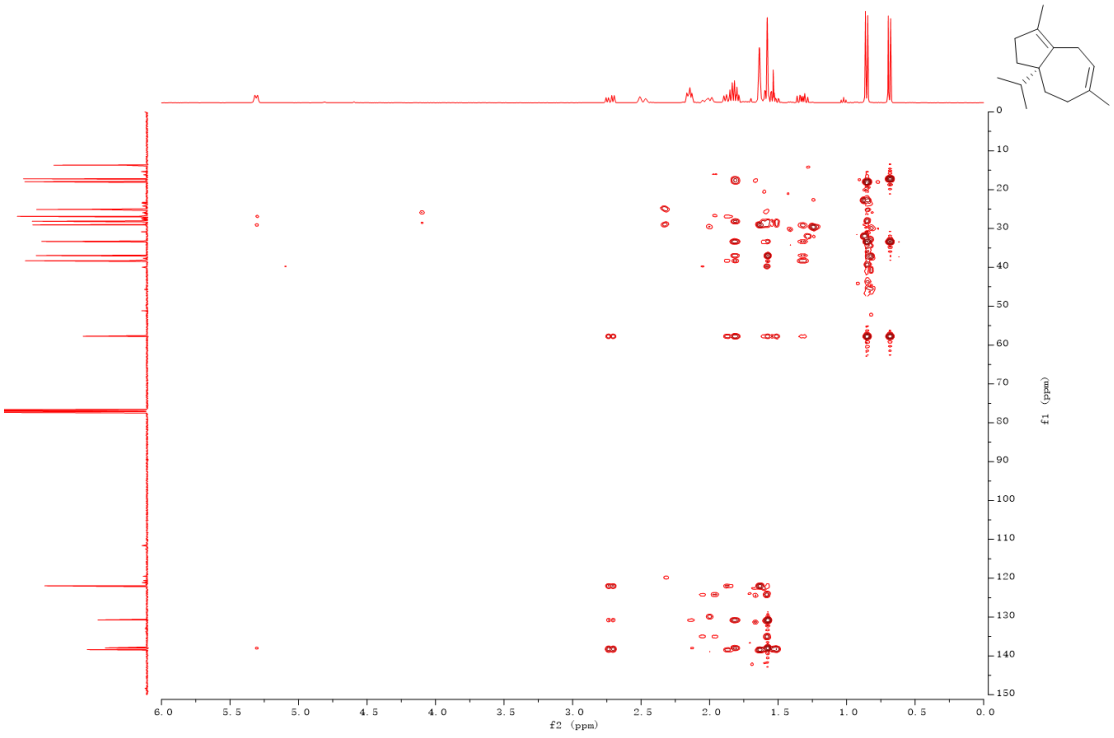

Figure S8e. HMBC spectrum of compound **1** in $CDCl_3$.

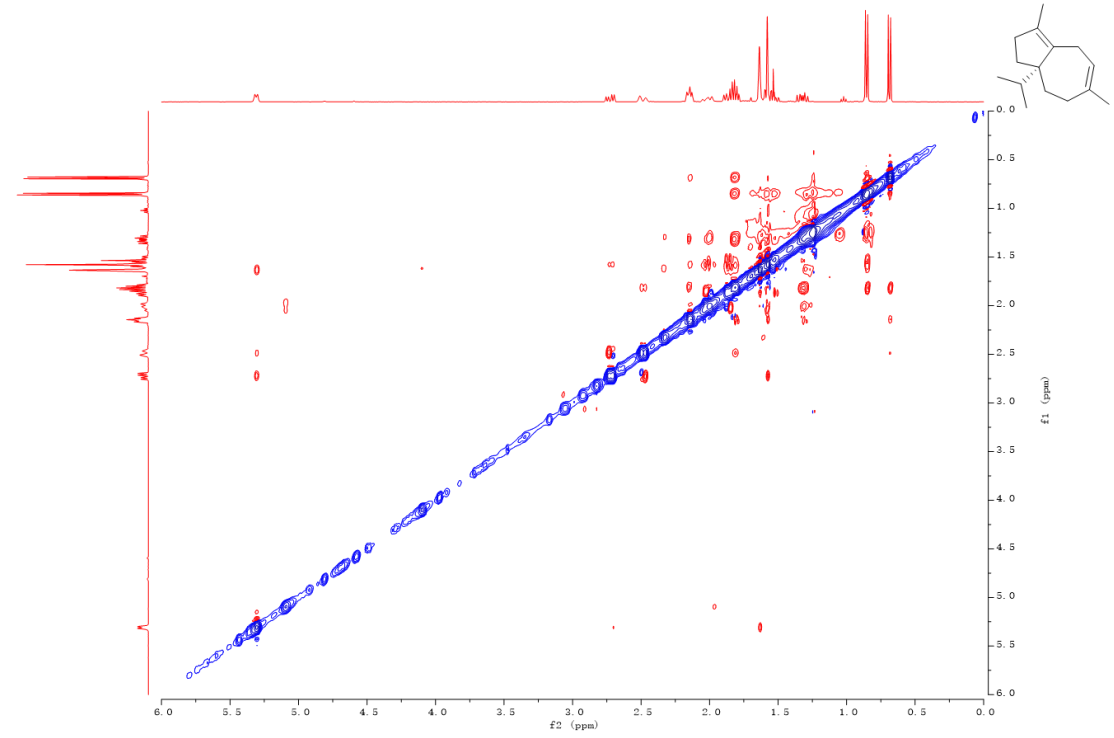

Figure S8f. NOESY spectrum of compound **1** in $CDCl_3$.

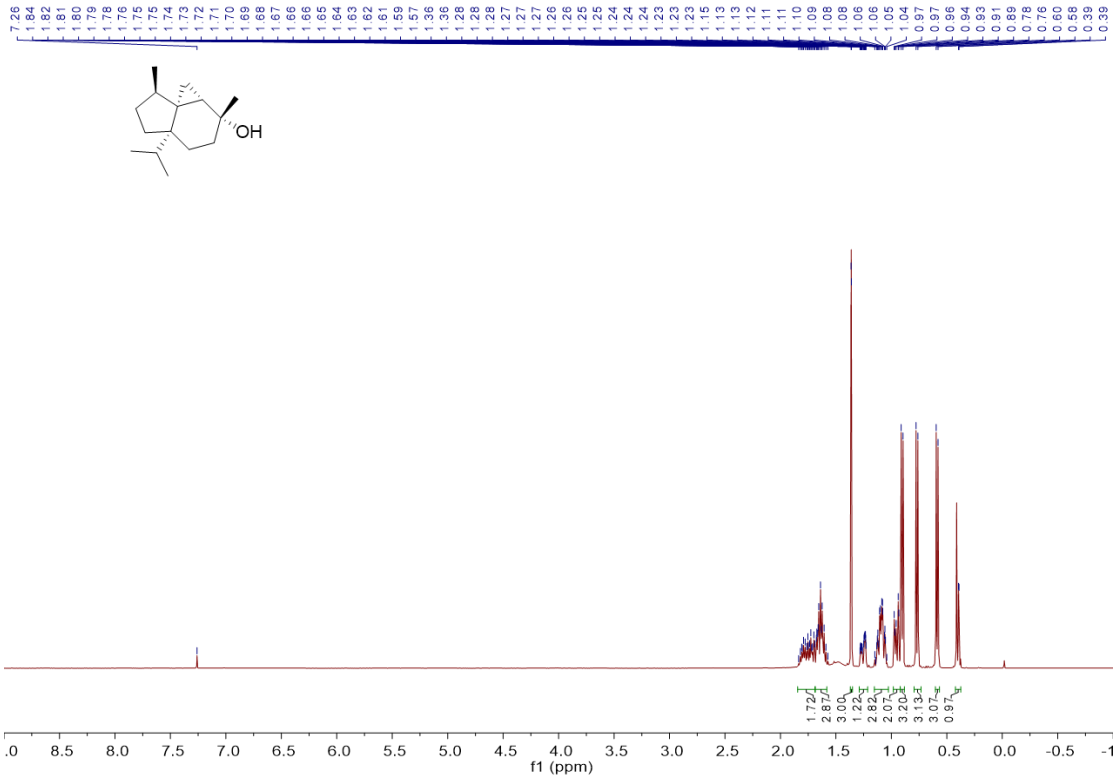

Figure S9a. ^{1}H NMR spectrum of compound **2** ($CDCl_3$, 400 MHz).

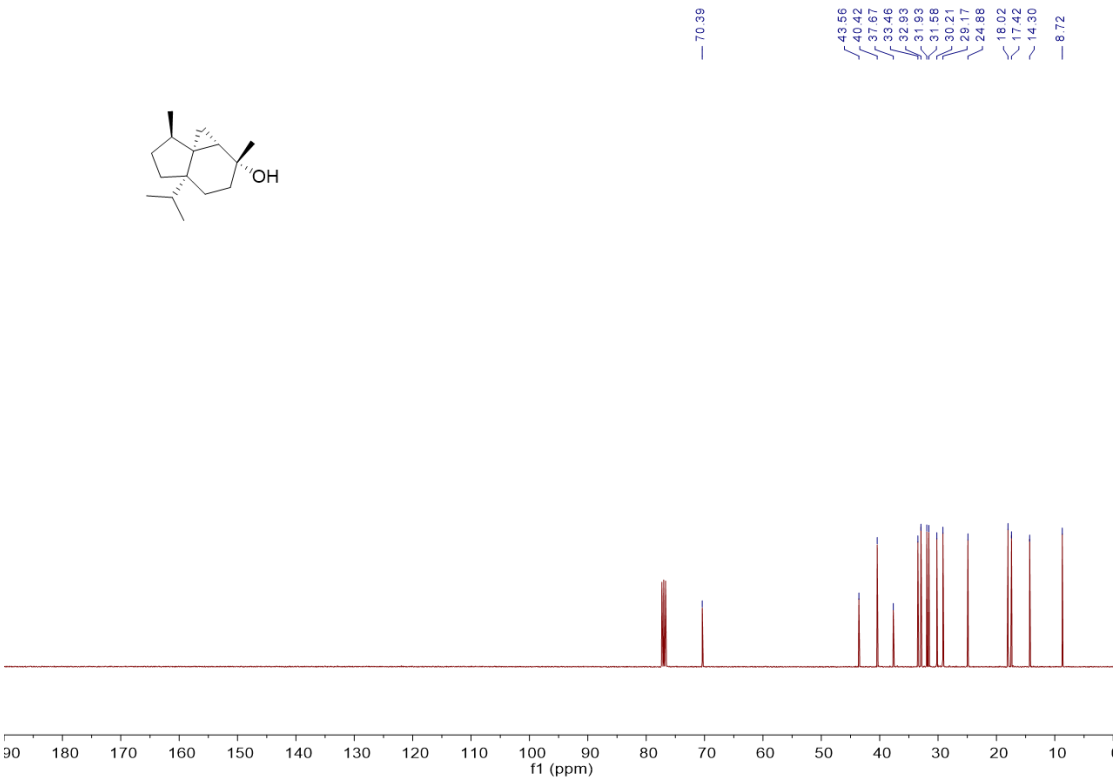

Figure S9b. ^{13}C NMR spectrum of compound **2** ($CDCl_3$, 101 MHz).

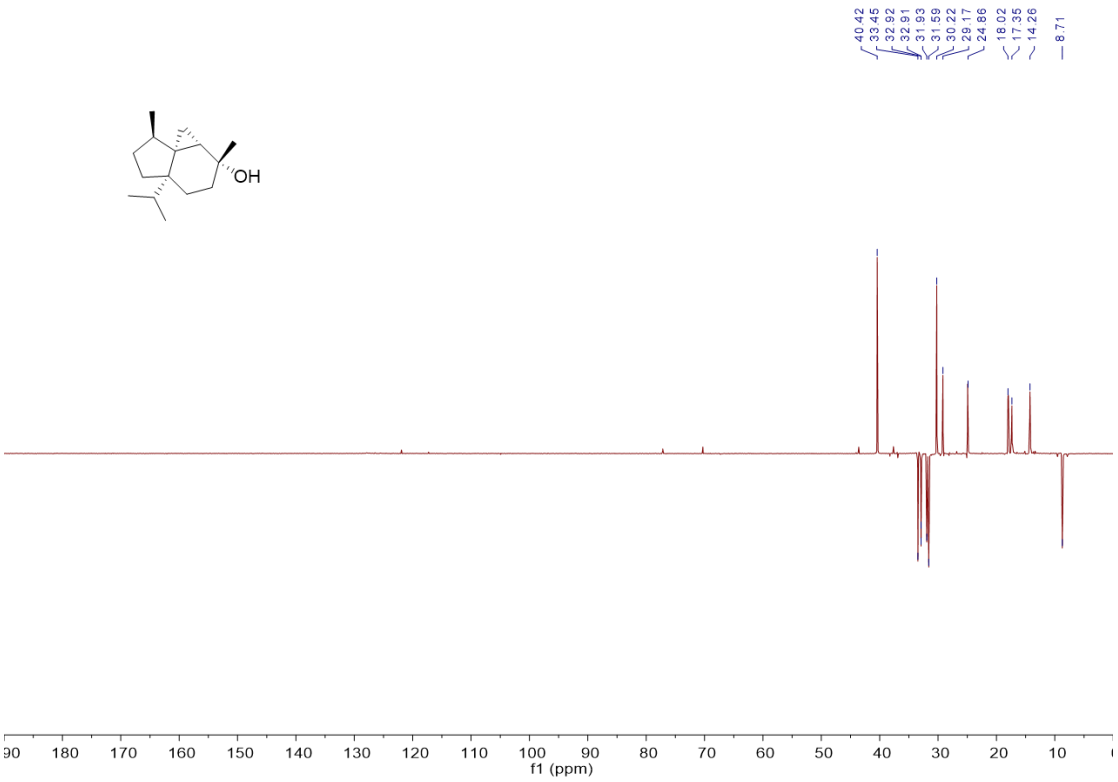

Figure S8c. DEPT135 spectrum of compound **2** ($CDCl_3$, 101 MHz).

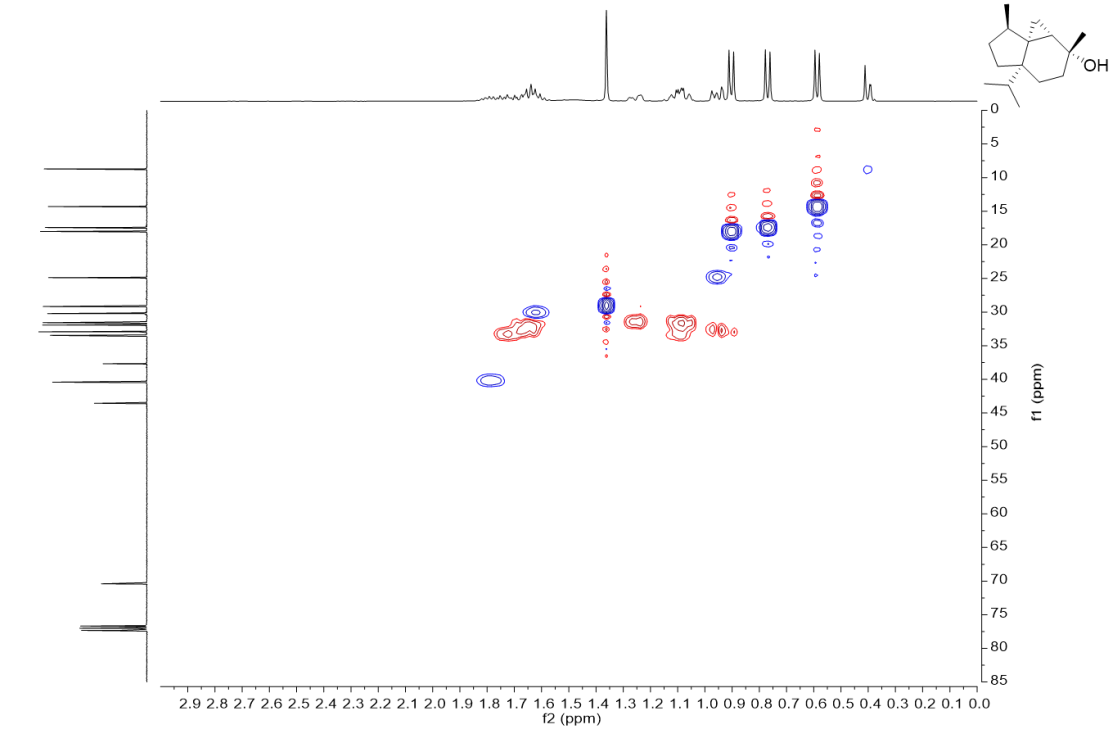

Figure S9d. HSQC spectrum of compound **2** in $CDCl_3$.

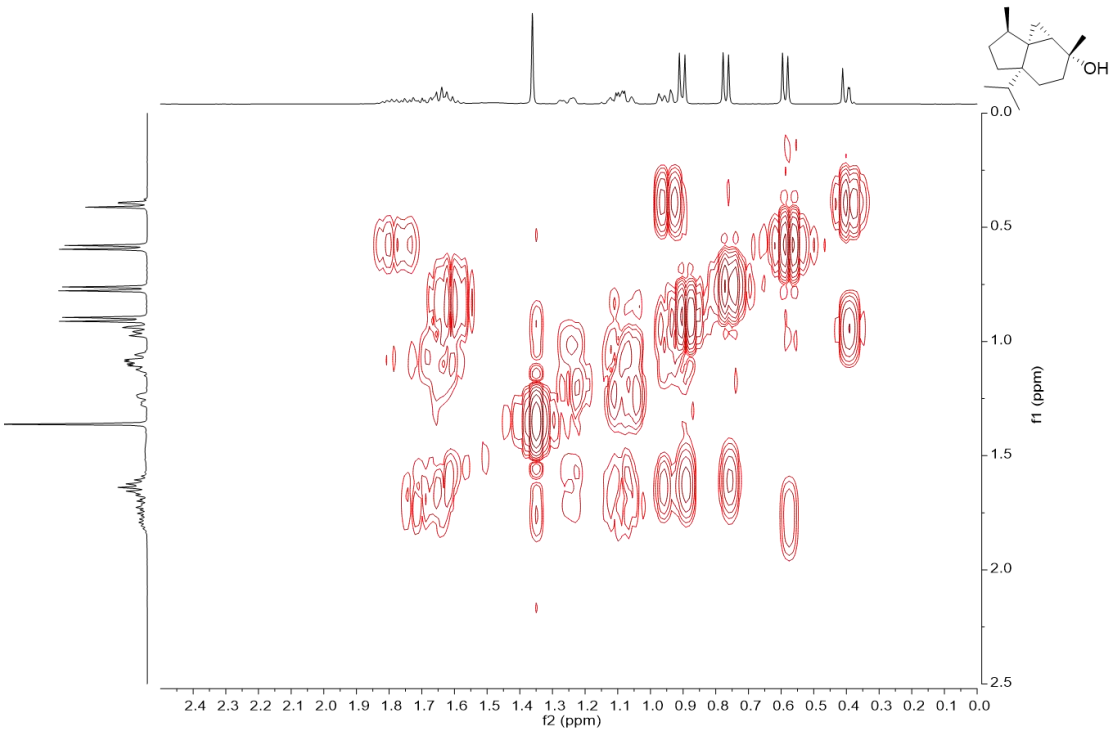

Figure S9e. ^{1}H-^{1}H COSY spectrum of compound **2** in $CDCl_3$.

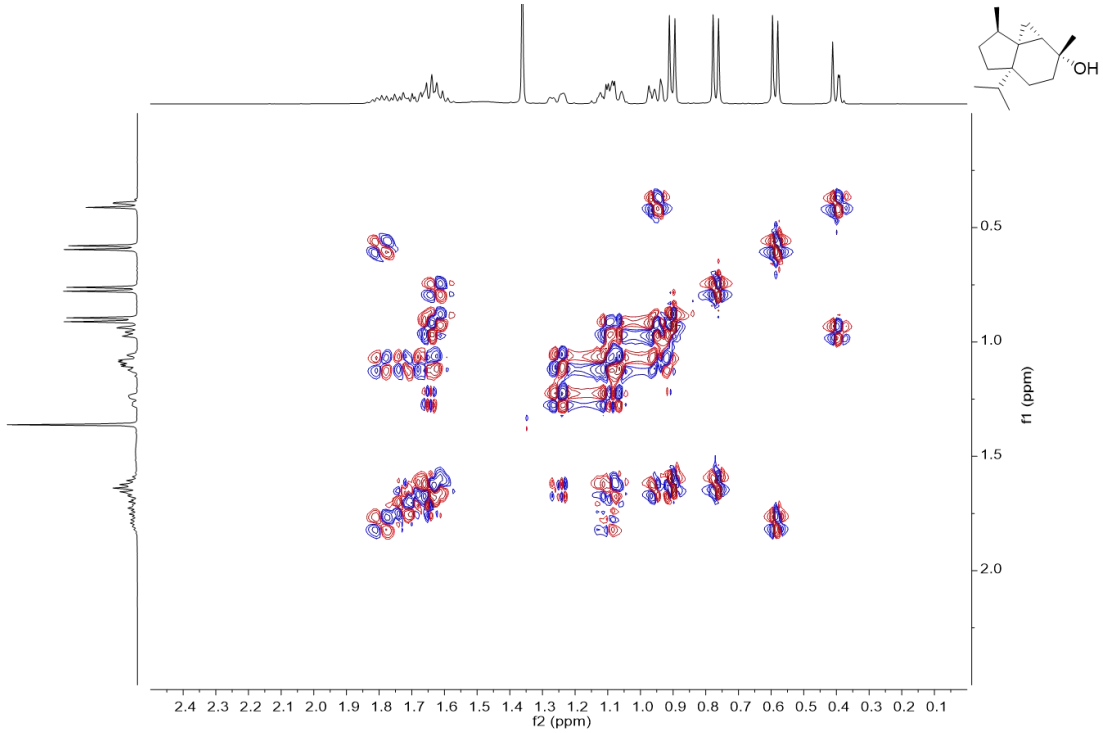

Figure S9f. DQF-COSY spectrum of compound **2** in $CDCl_3$.

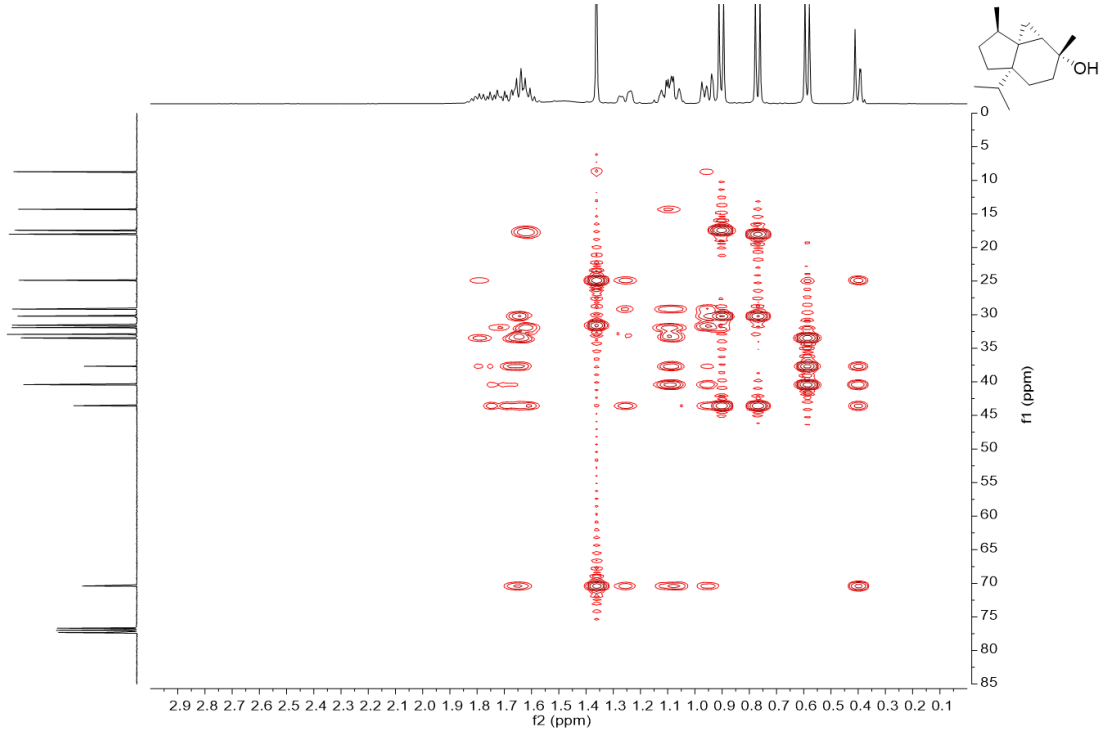

312

313 **Figure S9g.** HMBC spectrum of compound **2** in $CDCl_3$.

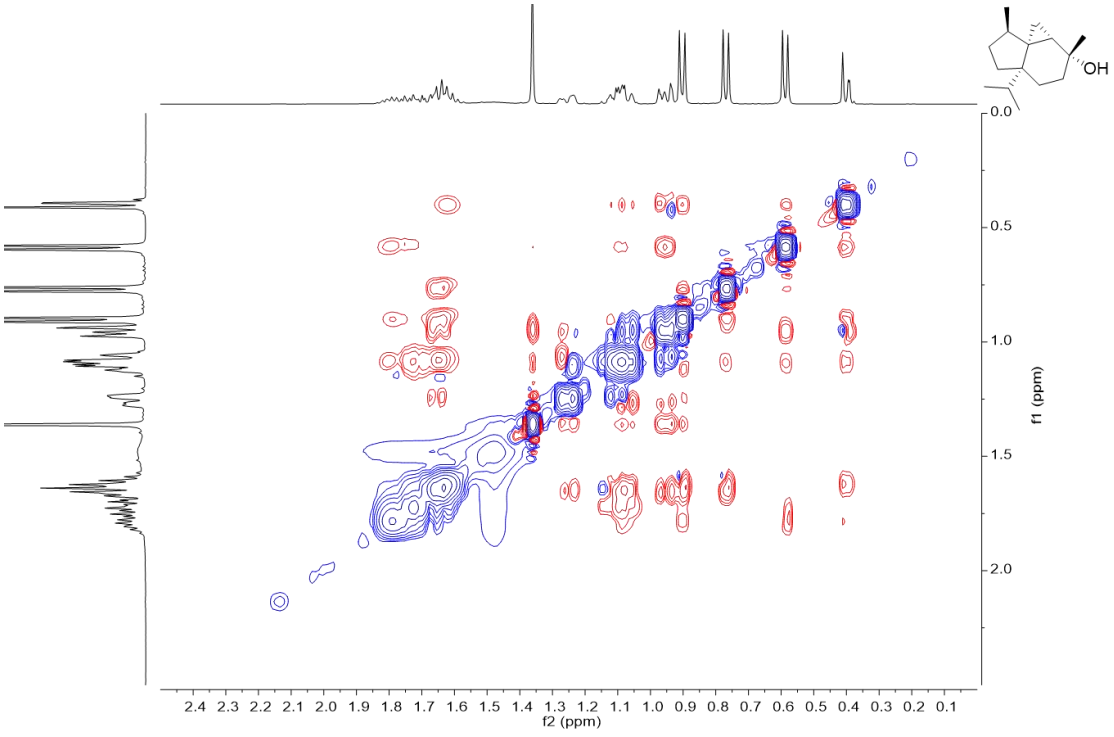

314

315 **Figure S9h.** NOESY spectrum of compound **2** in $CDCl_3$.

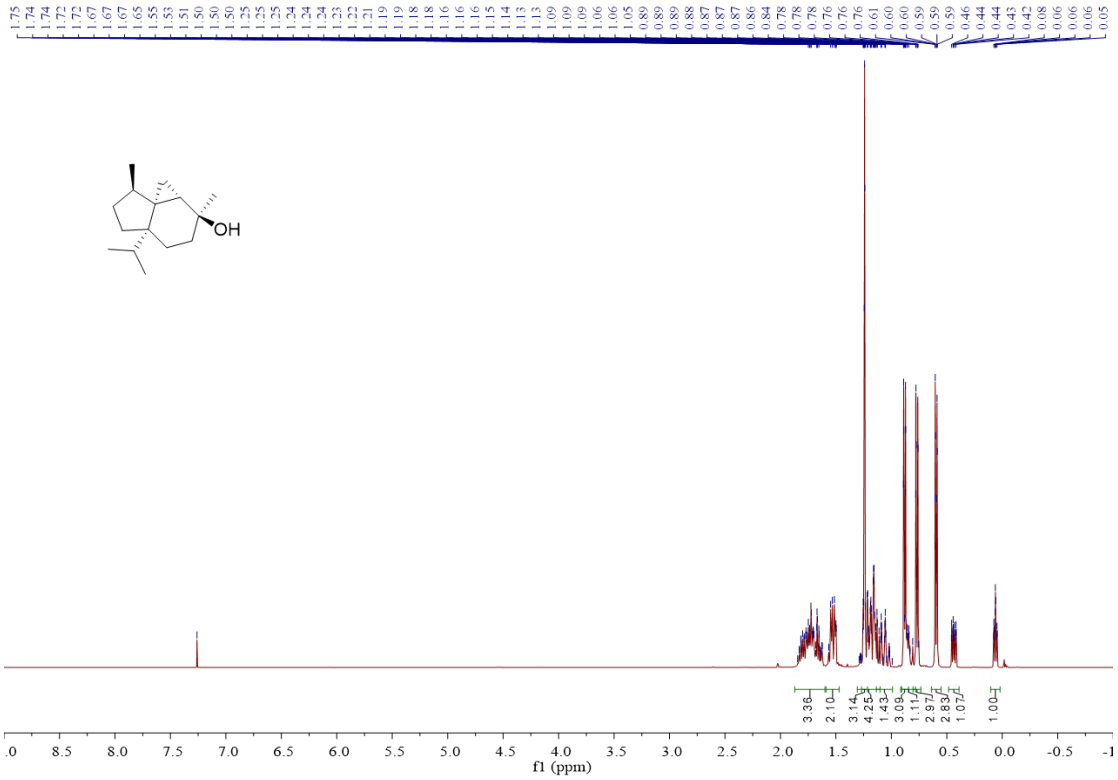

316

317 **Figure S10a**. ^{1}H NMR spectrum of compound **3** ($CDCl_3$, 400 MHz).

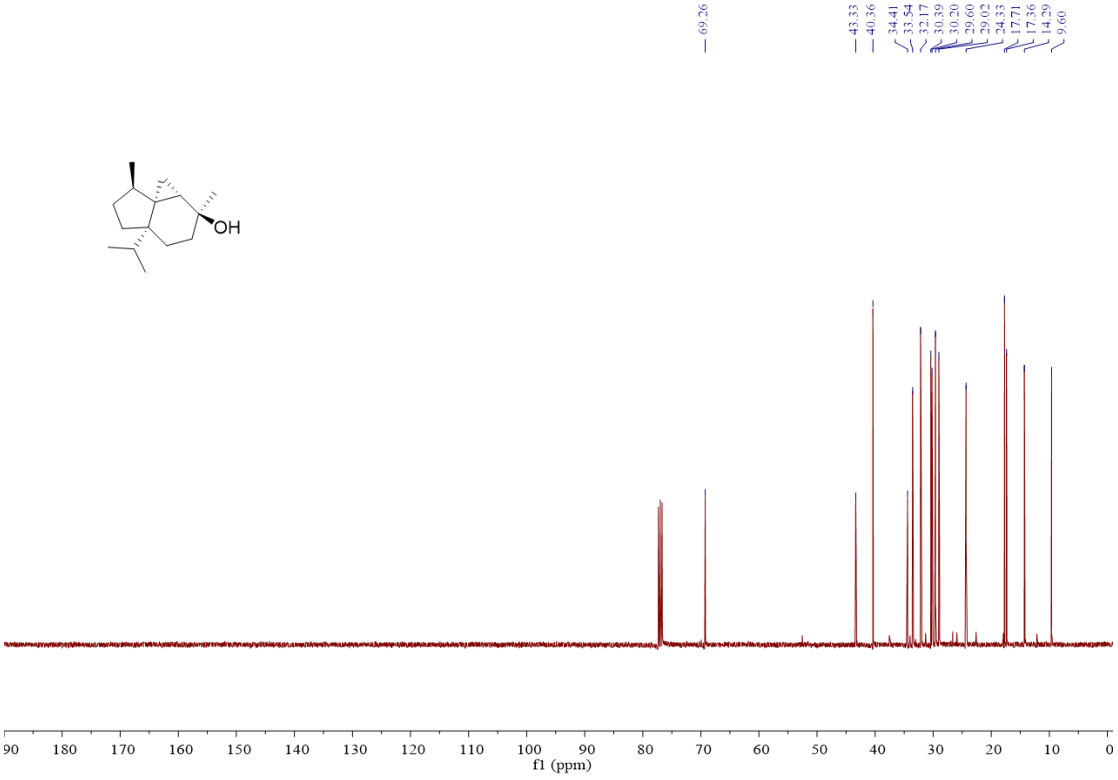

318

319 **Figure S10b.** ^{13}C NMR spectrum of compound **3** ($CDCl_3$, 101 MHz).

320

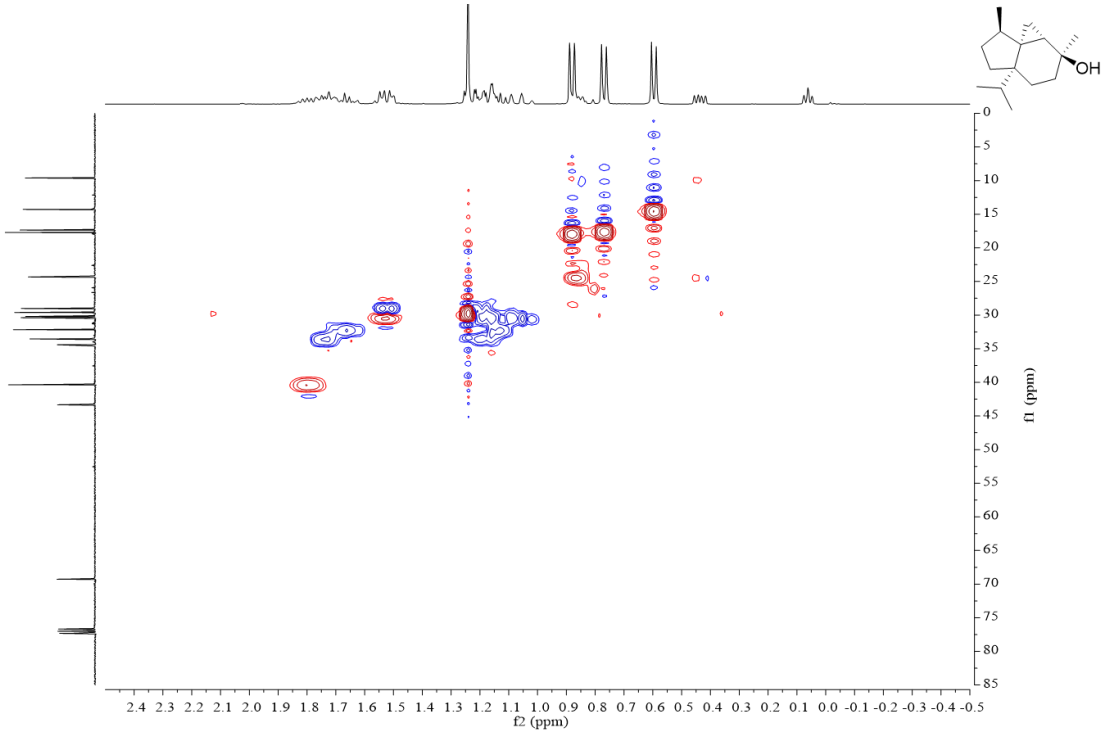

Figure S10c. HSQC spectrum of compound **3** in $CDCl_3$.

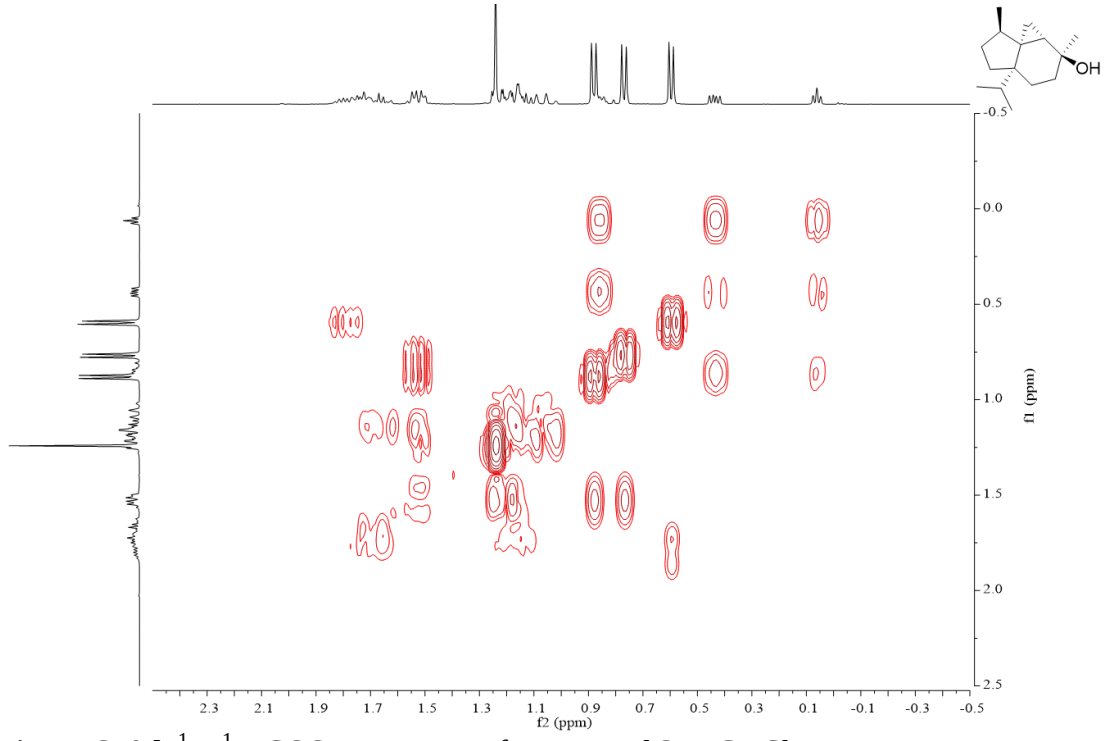

Figure S10d. ^{1}H-^{1}H COSY spectrum of compound **3** in $CDCl_3$.

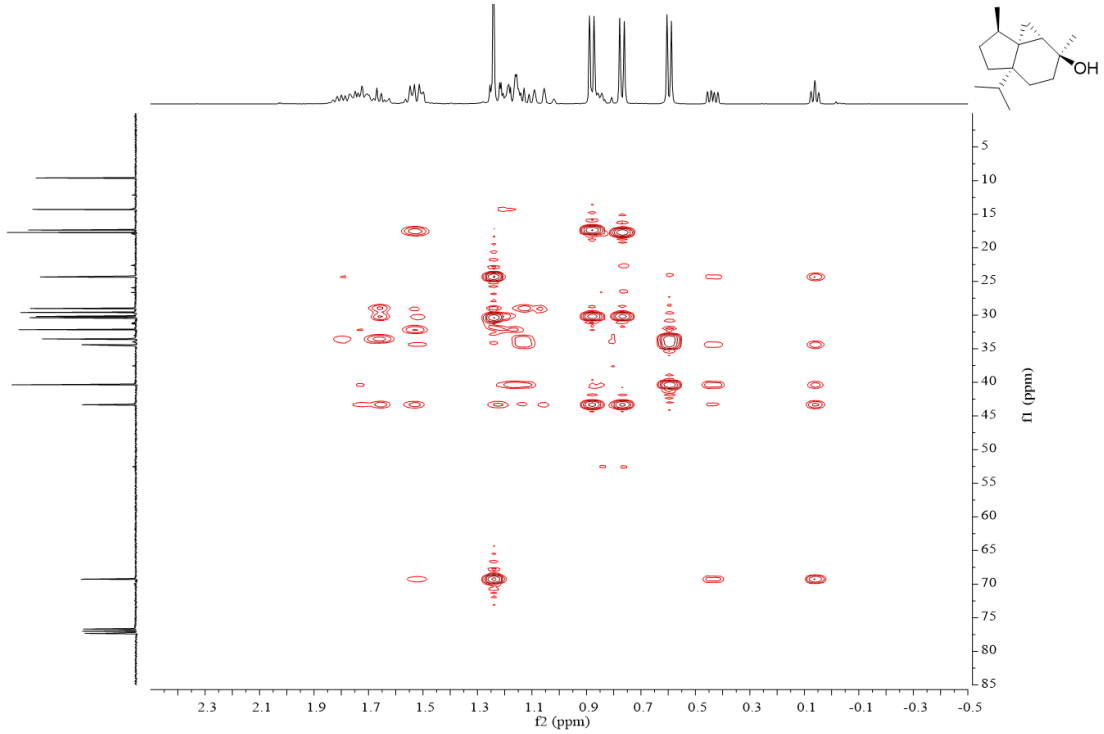

Figure S10e. HMBC spectrum of compound **3** in $CDCl_3$.

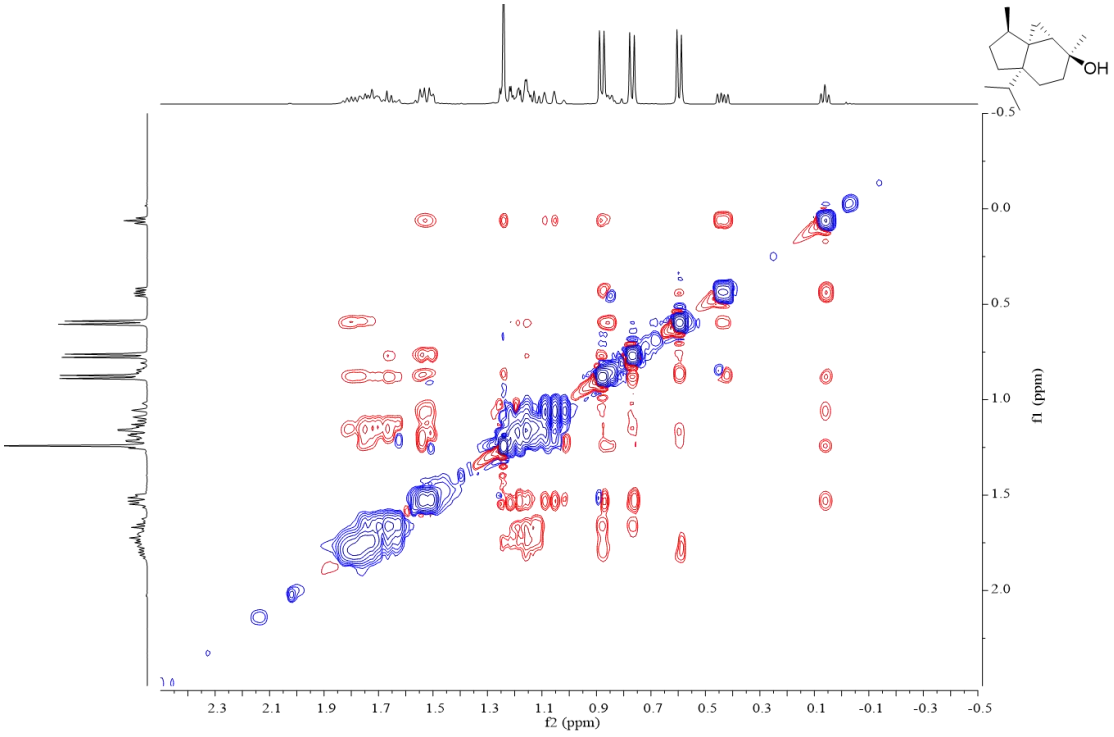

Figure S10f. NOESY spectrum of compound **3** in $CDCl_3$.

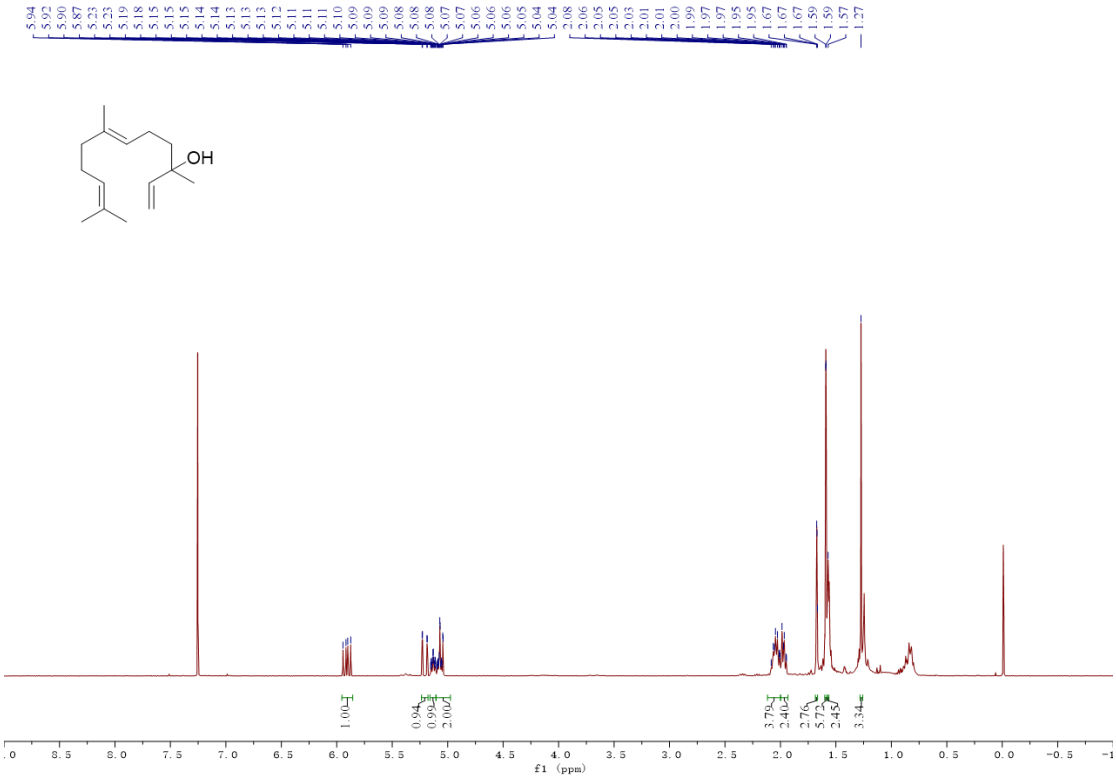

Figure S11a. ^{1}H NMR spectrum of compound **4** in $CDCl_3$.

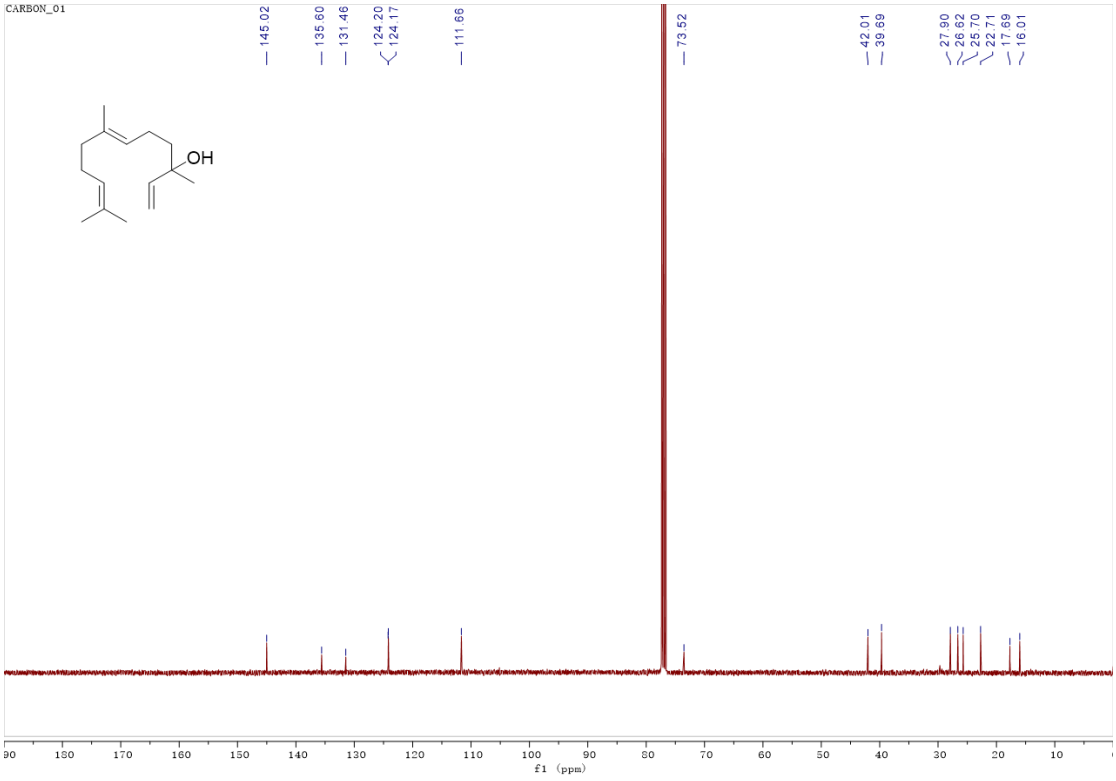

Figure S11b. ^{13}C NMR spectrum of compound **4** in $CDCl_3$.

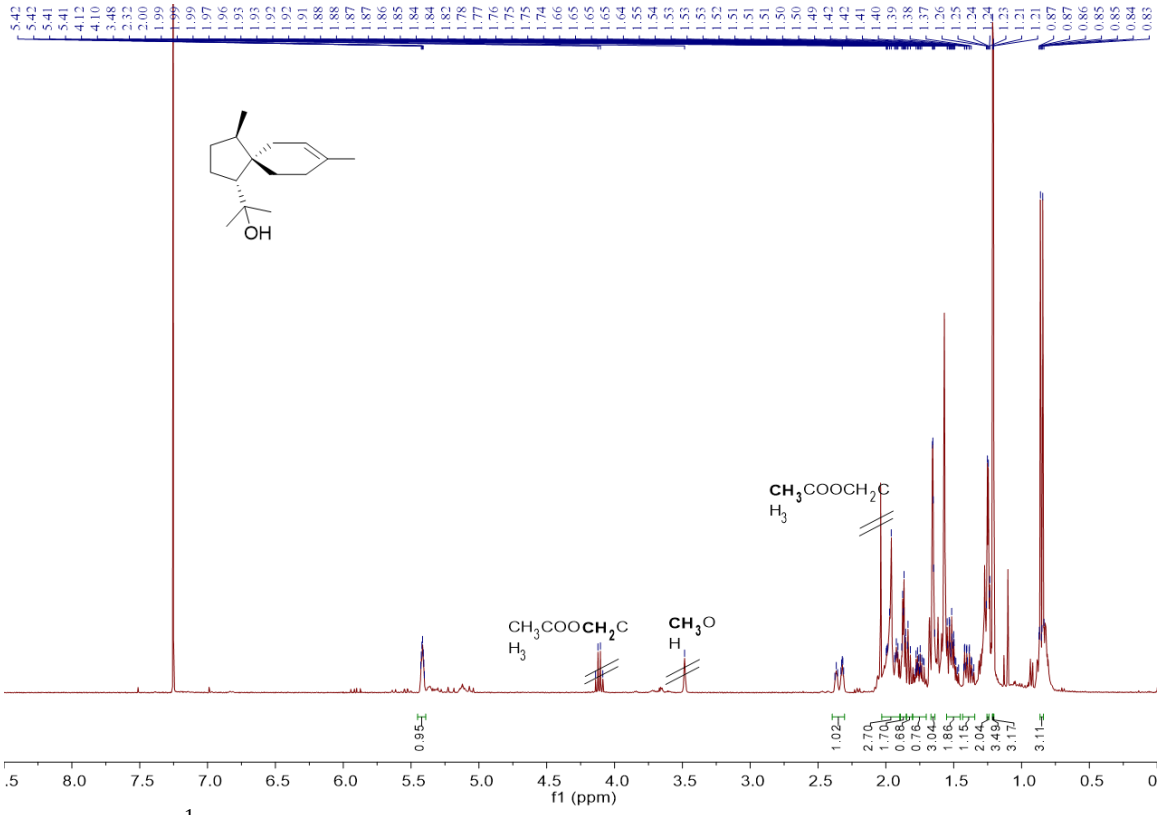

Figure S12a. ^{1}H NMR spectrum of compound **5** in $CDCl_3$.

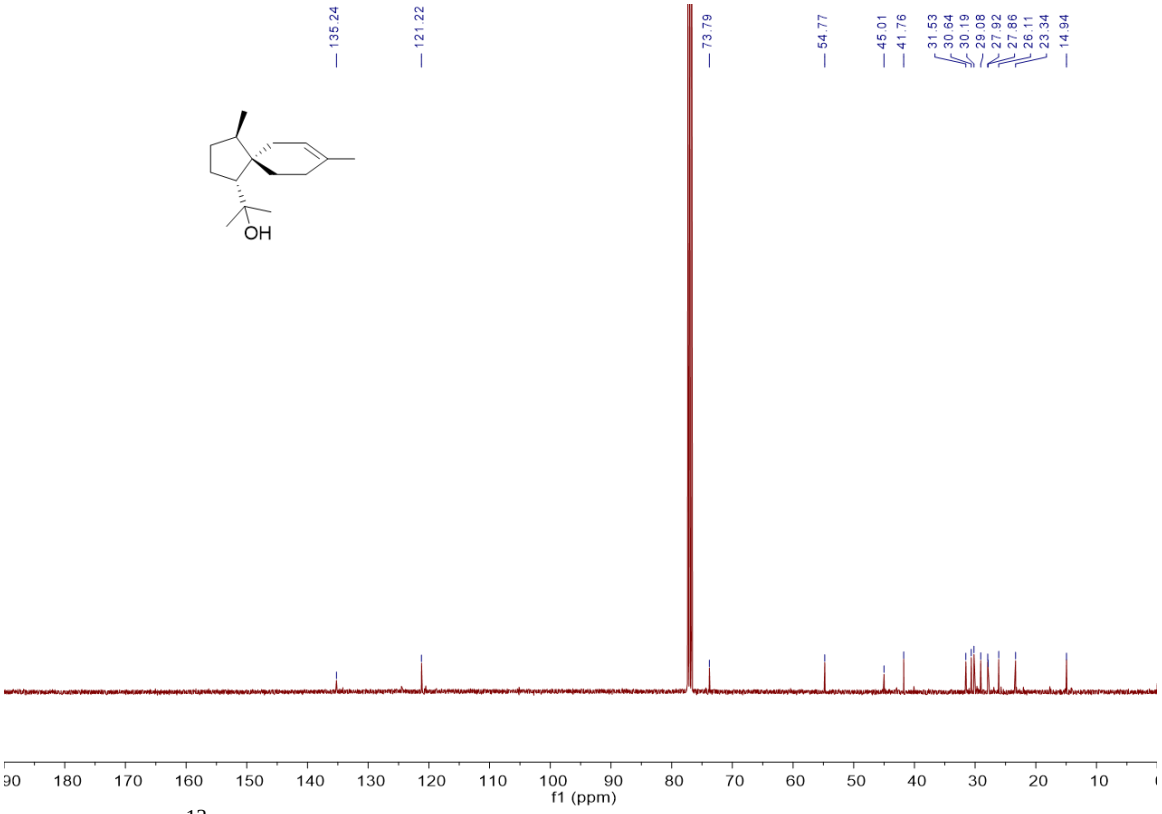

Figure S12b. ^{13}C NMR spectrum of compound **5** in $CDCl_3$.

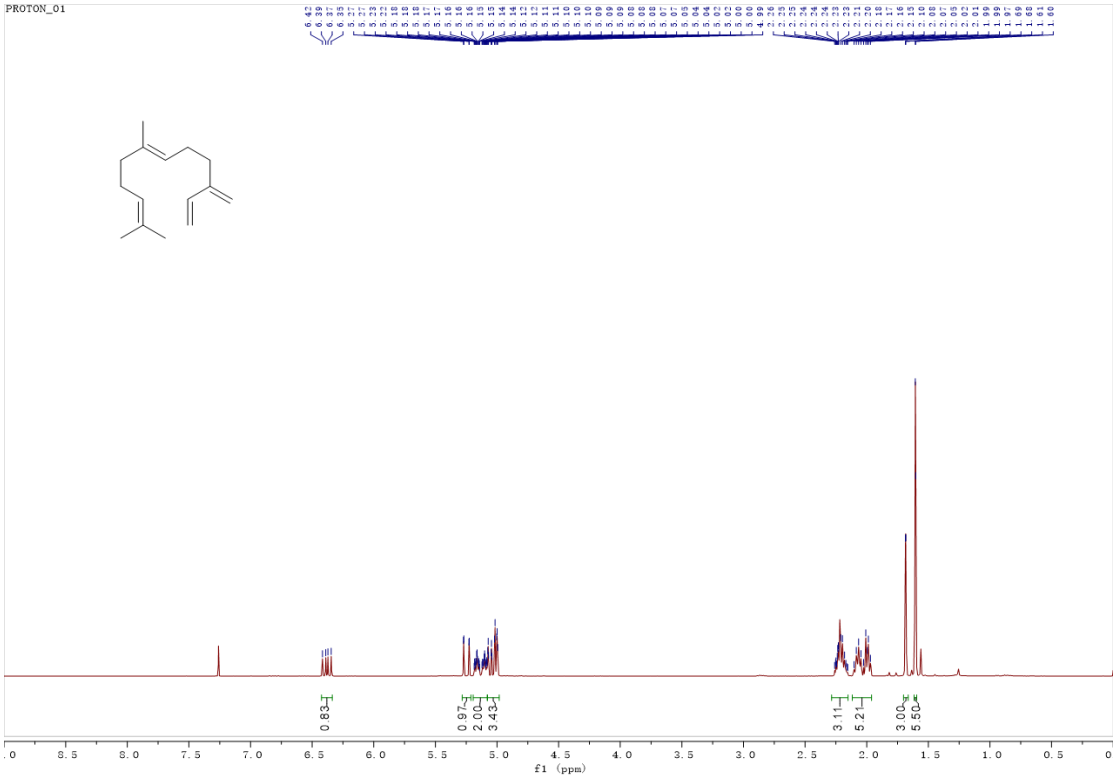

Figure S13a. ^{1}H NMR spectrum of compound **6** in $CDCl_3$.

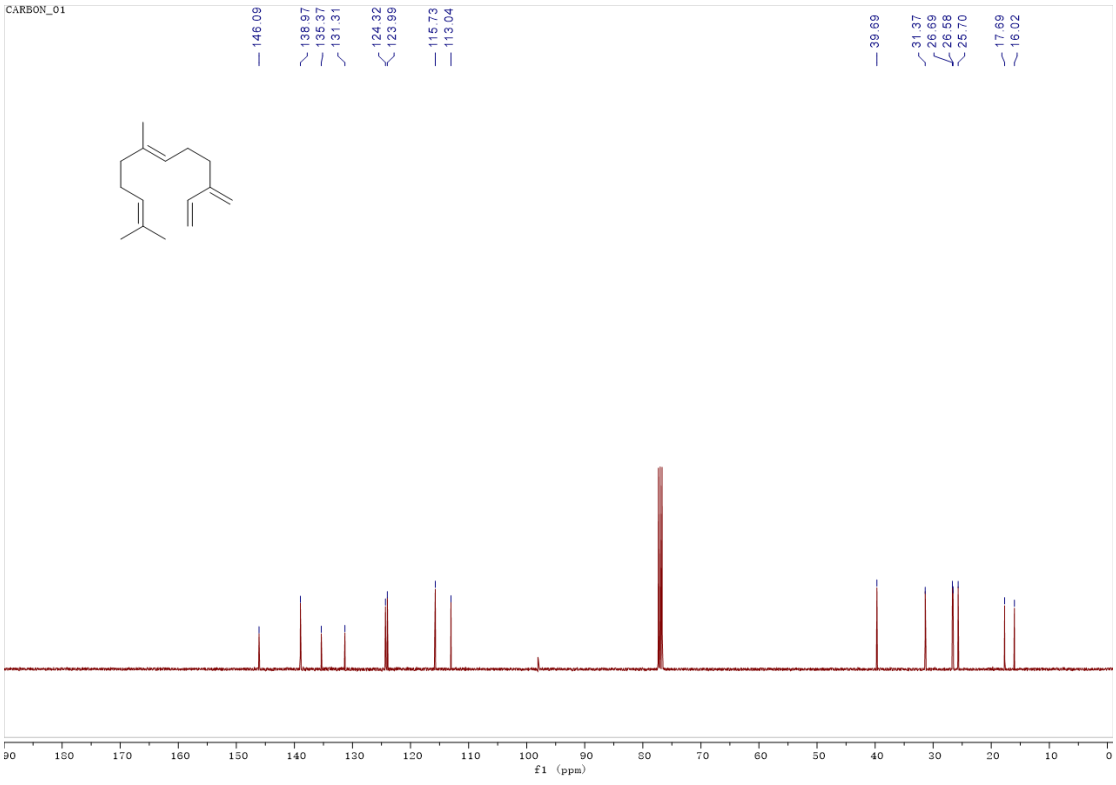

Figure S13b. ^{13}C NMR spectrum of compound **6** in $CDCl_3$.

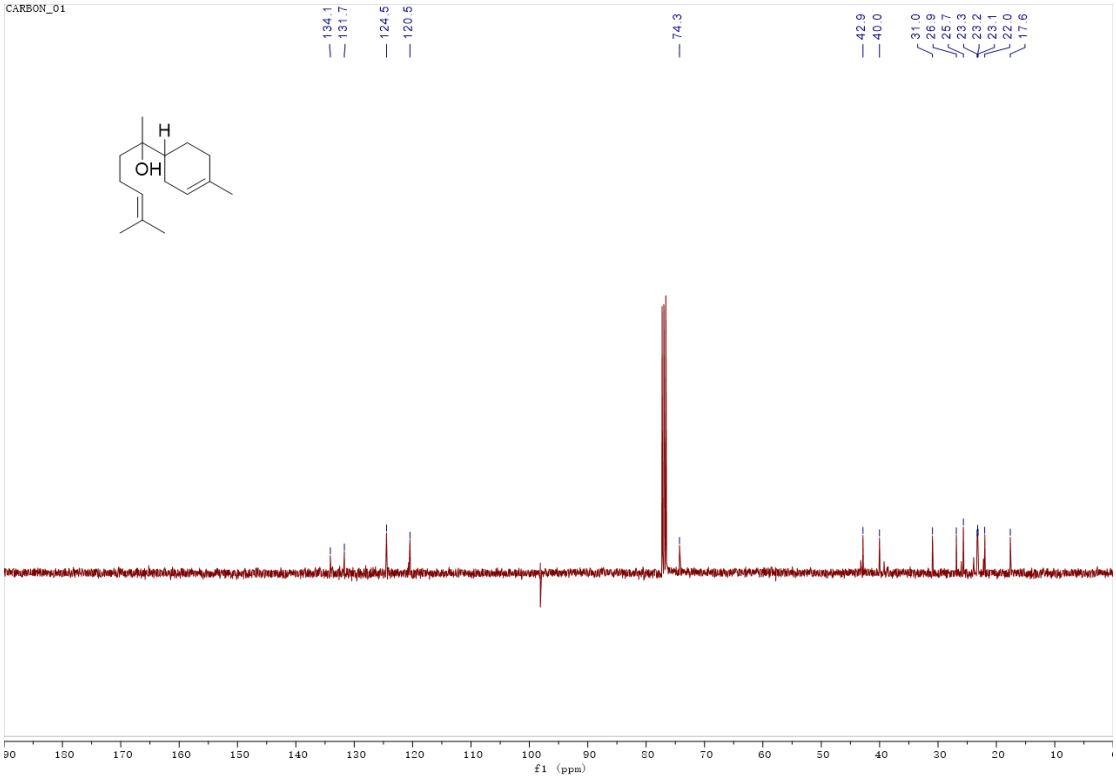

Figure S14. ^{13}C NMR spectrum of compound **7** in $CDCl_3$

.

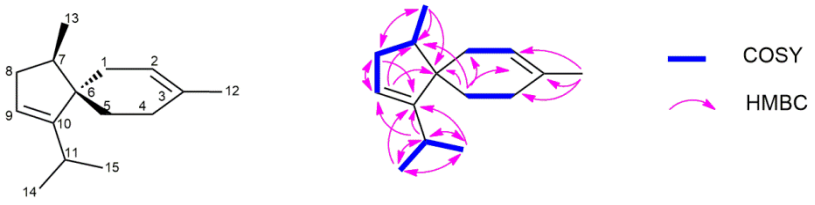

Figure S15a. The planar structure, ^{1}H-^{1}H COSY and the key HMBC correlations of compound **8**.

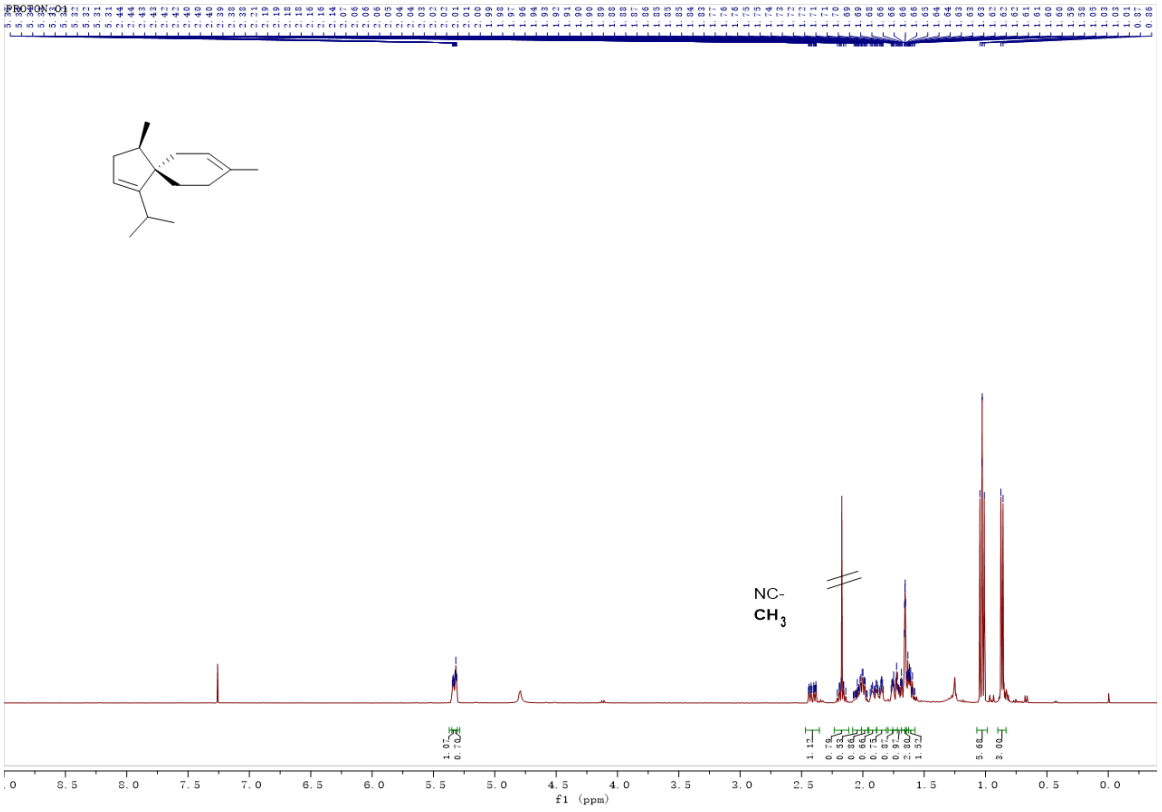

Figure S15b. ^{1}H NMR spectrum of compound **8** ($CDCl_3$, 400 MHz).

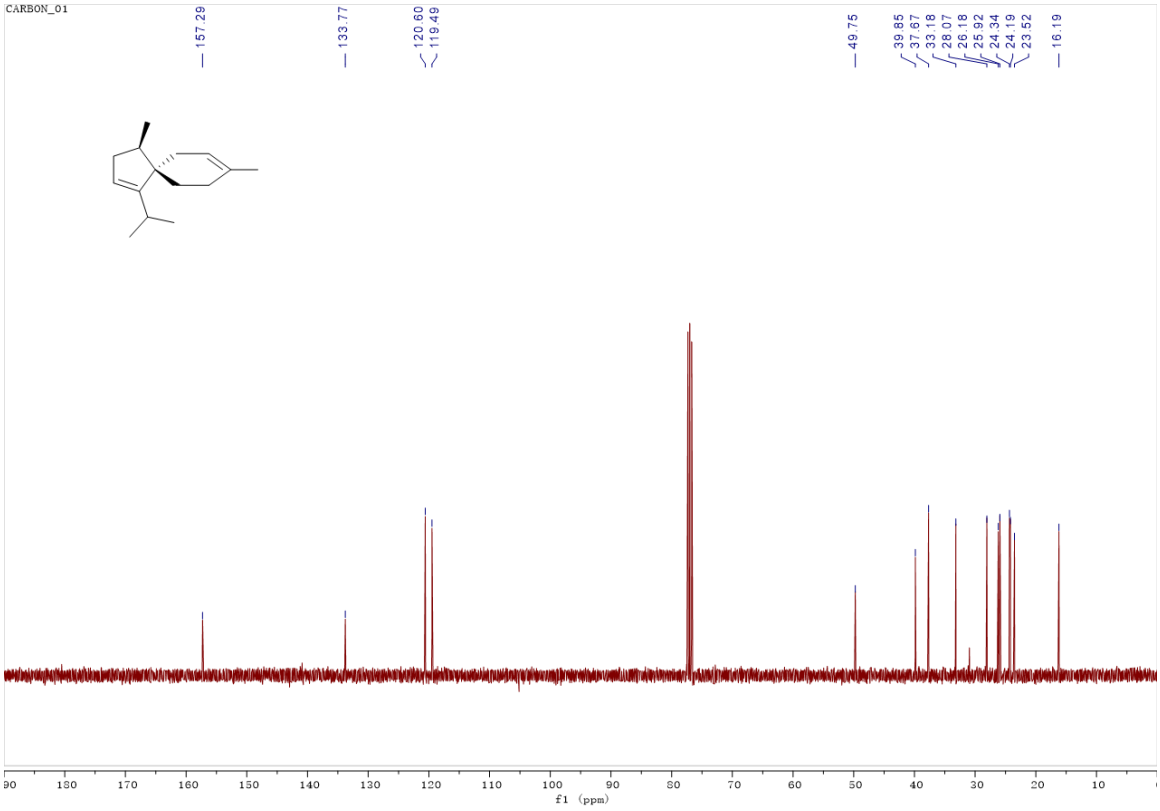

354

355 **Figure S15c.** ^{13}C NMR spectrum of compound **8** ($CDCl_3$, 101 MHz).

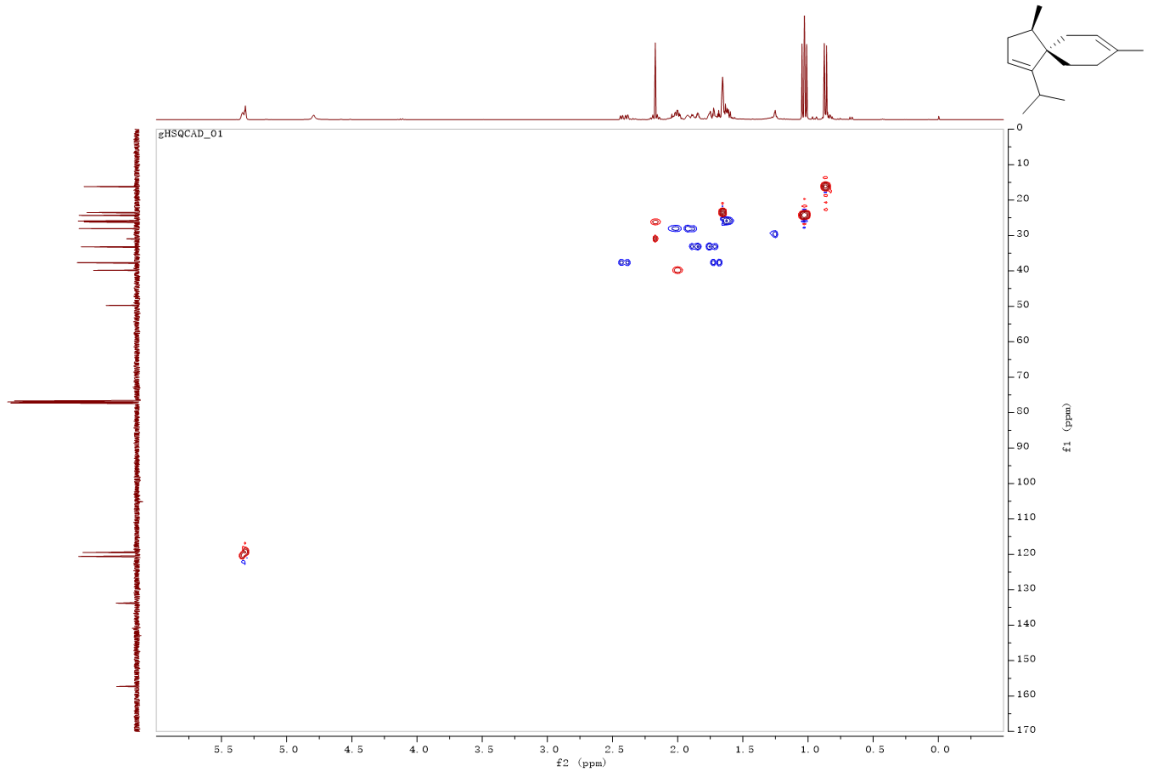

356

357 **Figure S15d.** HSQC spectrum of compound **8** in $CDCl_3$.

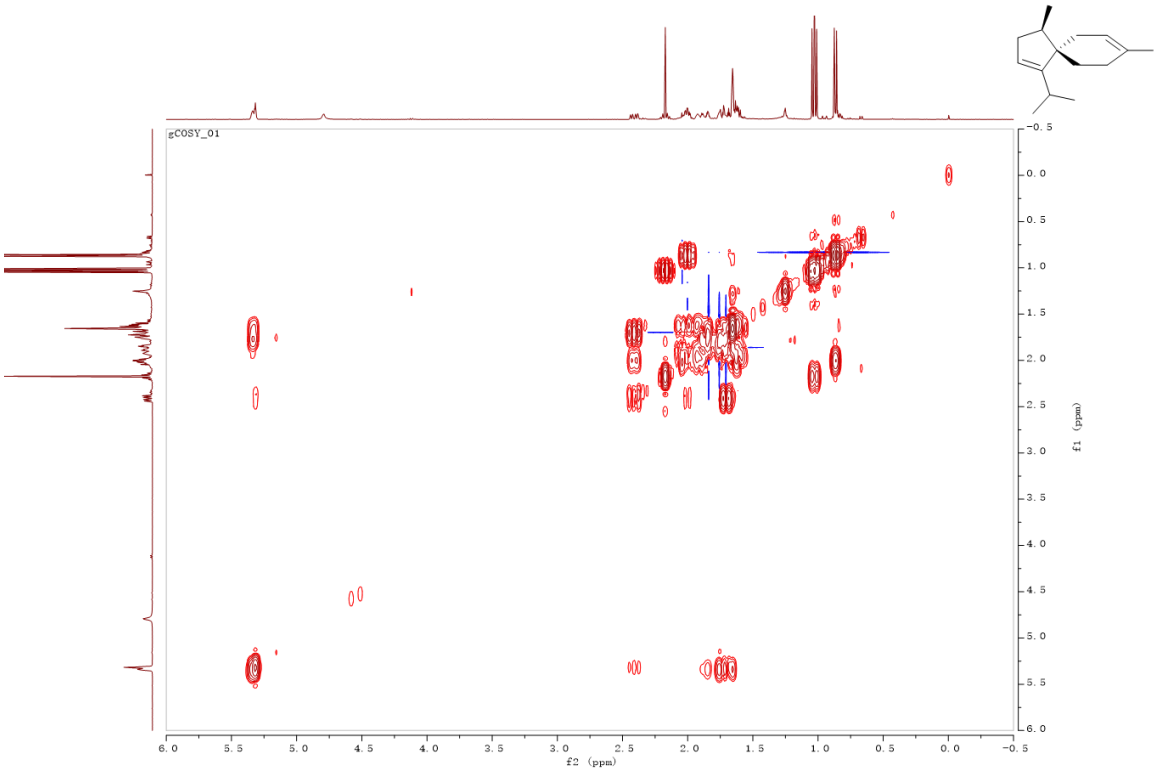

Figure S15e. ^{1}H-^{1}H COSY spectrum of compound **8** in $CDCl_3$.

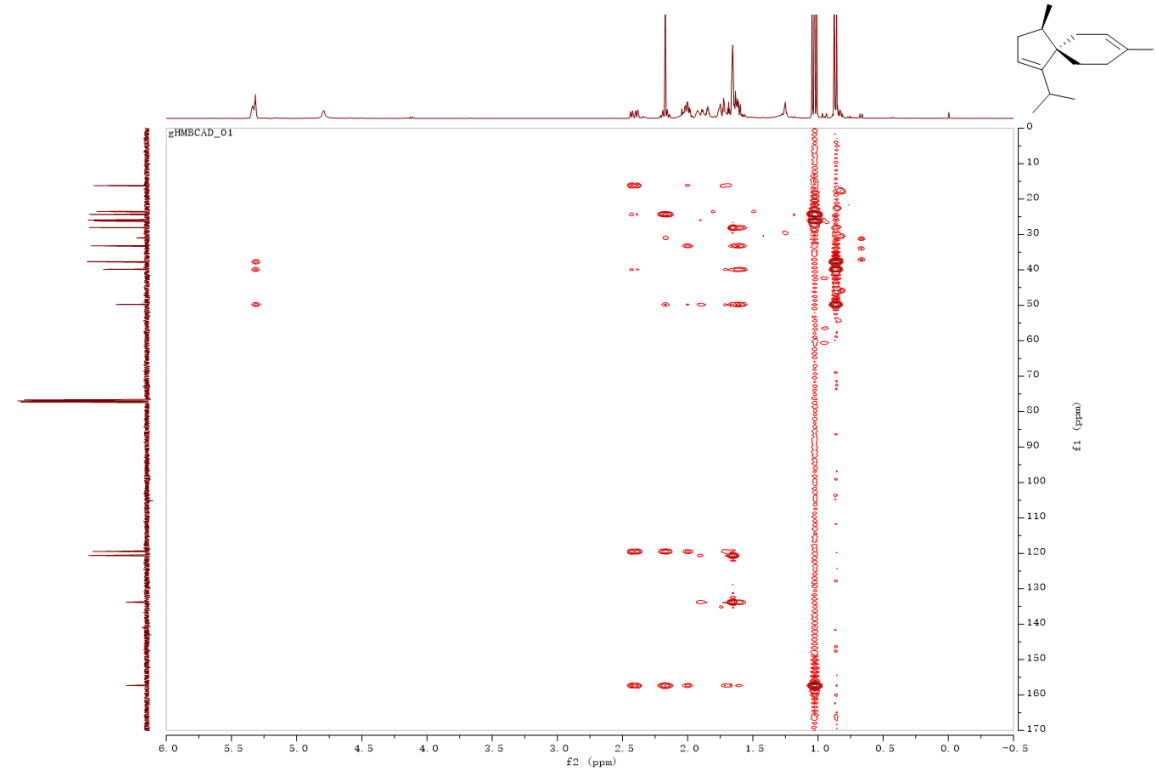

Figure S15f. HMBC spectrum of compound **8** in $CDCl_3$.

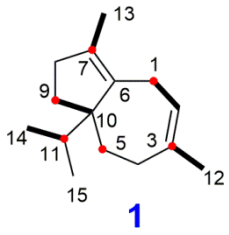

Figure S16. Compound **1** obtained from [1-^{13}C,$^{2}H_3$] sodium acetate feeding experiment.

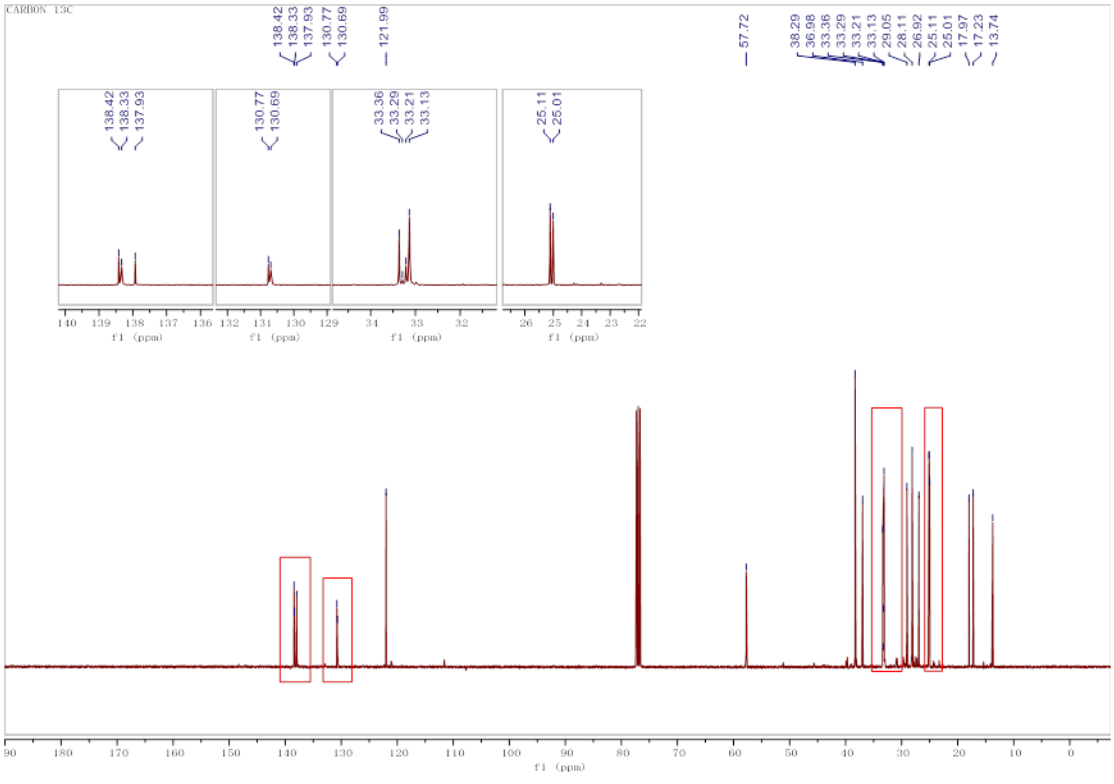

Figure S17. ^{13}C NMR spectrums of ^{13}C-labeled compound 1 ($CDCl_3$, 101 MHz).

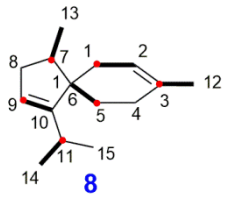

Figure S18. Compound **8** obtained from [1-^{13}C,$^{2}H_3$] sodium acetate feeding experiment.

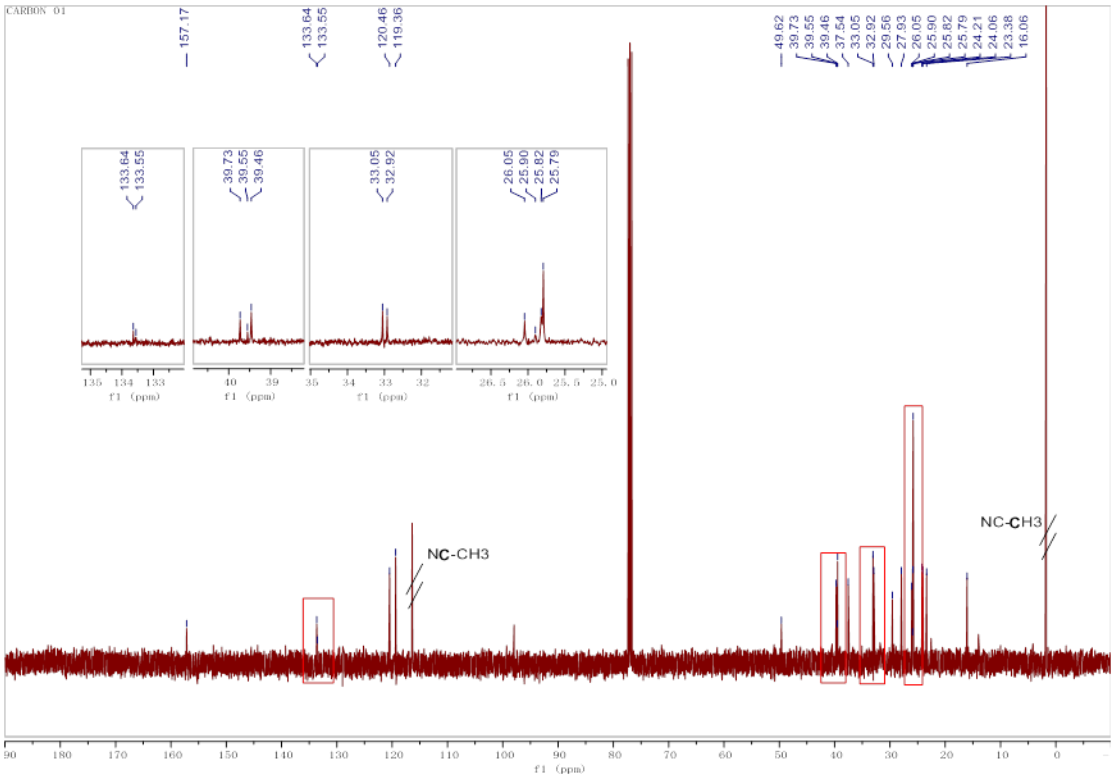

Figure S19. ^{13}C NMR spectrums of ^{13}C-labeled compound 8 ($CDCl_3$, 101 MHz).

Table S1. Oligonucleotides for the construction of plasmids used in this research.

No.	Primer name	Sequence 5'-3'
P1	1411 F	GCAATTAACCCTCACTAAAGGGAACAAAAGCGCGGCCGCttcaccgattctgagcgaat
P2	1411 R	GGCATCCGCTTACAGACAAGCTGTGAAAAGAAAGTGGAATATTCATTCATATCATATTT
P3	1417 F	AAAGAAGTGTCAAATCAAGTGTCAAATGTATACTTCTTTTTTTTACTTTGTTCAGAACA
P4	1417 R	AGCTCCCGGAGACGGTCACAGCTTGTCTGTGCGGCCGCttaatgatacgggagttgccg
P5	1416 F	acctctatactttaacgtcaaggagaaaaaactataGCGCAATGATTGAATAGTCAAAG
P6	1416 R	GTTGTTCTGAACAAAGTAAAAAAAAGAAGTATACATTTGACACTTGATTTGACACTTCT
P7	1412 F	GAAAAAATATGATATGAATGAATATTCCACTTTCTTTTCACAGCTTGTCTGTAAGCGG
P8	1412 R	GTGTTGATAAAAAATGTTTATCCATTGGACCGTGTAGTACCCAATTCGCCCTATAGTGA
P9	1413 F	GCGCGTAATACGACTCACTATAGGGCGAATTGGGTACTACACGGTCCAATGGATAAACA
P10	1413 R	ATCGTTTGAAAGATGGGTCCGTCACCTGCATTAAATCCTAATCTCTGCTTTTGTGCGCG
P11	1414 F	GTACATACATAAACATACGCGCACAAAAGCAGAGATTAGGATTTAATGCAGGTGACGGA
P12	1414 R	aaaaaagtaagaatttttgaaaattcaatataaATGGTTTTAACCAATAAAACAGTCAT
P13	1415 F	AAATGACTGTTTTATTGGTTAAAACCATttatattgaattttcaaaaattcttactttt
P14	1415 R	AAAAAAATCTTTGACTATTCAATCATTGCGCtatagttttttctccttgacgttaaagt
P15	1418 F	gcttatattgcggcaactcccgtatcattaaGCGGCCGCACAGACAAGCTGTGACCGTC
P16	1418 R	acctgtgattcgctcagaatcggtgaaGCGGCCGCGCTTTTGTTCCCTTTAGTGAGGGT
P17	FgJ03939 F (NdeI)	ATATCATATGCCTCACAAGCACGTTCCTC
P18	FgJ03939 R (EcoRI)	ATATGGTGACCGAATTCCTAACACTTGCAAGGAAGTGGTC
P19	3939-Tadh1 GF	CATAAATCATAAGAAATTCGCCTAACACTTGCAAGGAAGTGG
P20	3939-Pgal1-10 R	GAAAATTCAATATAAGCCACCATGCCTCACAAGCACGTTC
P21	Pgal1-10-3939 F	GTGAGGCATGGTGGCTTATATTGAATTTTCAAAAATTC
P22	Pgal1-10-ERG20 R	CTGAAGCCATGGTGGCTATAGTTTTTTCTCCTTGACG
P23	ERG20-Pgal1-10 F	GAGAAAAAACTATAGCCACCATGGCTTCAGAAAAAGAAATTAG
P24	ERG20-Tcyc GR	GTGACATAACTAATTACATGACTATTTGCTTCTCTTGTAAAC
P25	Tcyc-ERG20 GF	GTTTACAAGAGAAGCAAATAGTCATGTAATTAGTTATGTCAC
P26	Tadh1-3939 GR	CCACTTCCTTGCAAGTGTTAGGCGAATTTCTTATGATTTATG

Table S2. Strains and plasmids used in this research.

Strains	**Relevant genotype**	**Reference**
BL21 (DE3)	*E. coli B F⁻dcm ompT hsdSB(rB⁻mB⁻)gal*	Invitrogen
CEN.PK2-1D	*Saccharomyces cerevisiae* MATalpha; his3D1; leu2-3_112; ura3-52; trp1-289; MAL2-8c; SUC2	EUROSCARF
J1-012	*Fusarium graminearum*	This work
YZL141	*S. cerevisiae*:: *pGAL10-tHMG1*	This work
T16	*S. cerevisiae*:: P_{GAL10}-*tHMG1;* P_{GAL10}-*FgJ03939*; P_{GAL1}-*ERG20*	This work
Plasmids	**Description**	**Reference**
pZY141	pRS426 derived, *TRP1*, P_{GAL10}-*tHMG1*-T_{ACT1}	This work
pGB152	pET28a derived, P_{T7}: N-terminal his_6-tag FgJ03939	This work
pGB315	p426gal derived, *URA*, T_{CYC1}-ERG20-P_{GAL1}-P_{GAL10}-FgJ03939-T_{ADH1}	This work

382 **Table S3.** Kinetic constants of FgJ03939 with GPP, FPP and GGPP.

383

Substrate	FgJ03939		
	k_m [μM]	k_{cat} [s^{-1}]	k_{cat}/k_m [M^{-1} s^{-1}]
GPP	9.9±1.23	(17±0. 4)×10^{-3}	1.7×10^3
FPP	16.396±3.277	(94.5±9.1)×10^{-3}	5.8×10^3
GGPP	5.9257±1.559	(16±1)×10^{-3}	2.7×10^3

384 **Table S4.** ^{1}H and ^{13}C NMR data of compound **1** ($CDCl_3$, 400 MHz and 101 MHz).

Position	^{13}C	^{1}H				
	δ(ppm)	δ(ppm)	Intensity	Multiplicity	HMBC correlation	COSY correlation
1	25.11	2.72	1H	dd (*J* = 16.7, 7.4 Hz)	2, 3, 6, 7, 10	H-1b, H-2
		2.48	1H	d (*J* = 16.9 Hz)		H-1a
2	121.98	5.30	1H	m	1, 4,12	H-1a
3	138.39					
4	29.06	2.01	1H	m	2, 3, 5, 10, 12	
		1.85	1H	m		H-5b
5	38.29	1.59	1H	m		
		1.52	1H	m	3, 6, 10	H-4b
6	137.93					
7	130.74					
8	36.96	2.15	2H	m		H-9b
9	28.13	1.81	1H	m		H-9b
		1.32	1H	m	8, 10, 11	H-8, H-9a
10	57.72					
11	33.34	1.81	1H	m		H-14, H-15
12	26.88	1.63	3H	s	2, 3, 4	
13	13.71	1.58	3H	s	6, 7, 8	
14	17.96	0.68	3H	d (*J* = 6.8 Hz)	10, 11, 15	H-11
15	17.21	0.86	3H	d (*J* = 6.8 Hz)	10, 11, 14	H-11

Table S5. ^{1}H and ^{13}C NMR data of compound **2** ($CDCl_3$, 400 MHz and 101 MHz).

Position	^{13}C	^{1}H				
	δ(ppm)	δ(ppm)	Intensity	Multiplicity	HMBC correlation	COSY correlation
1	8.72	0.39	2H	m	2, 3, 6, 7, 10	H-2
2	24.88	0.95	1H	m		H-1
3	70.39					
4	31.58	1.25	1H	d (*J* = 13.2 Hz)	2, 3, 10, 12	H-4b, H-5β
		1.08	1H	m		H-4a, H-5α
5	32.93	1.66(β)	1H	m		H-5α
		0.94(α)	1H	m		H-4b, H-5β
6	37.67					
7	40.42	1.79	1H	m	2, 6, 8, 13	H-8b, H-13
8	33.46	1.71	1H	m	7, 9, 10	
		1.09	1H	m		H-7
9	31.93	1.64	1H	m		H-9b
		1.07	1H	m		H-9a
10	43.56					
11	30.21	1.62	1H	m	9, 14, 15	H-14, H-15
12	29.17	1.36	3H	s	4, 3, 4	
13	14.3	0.59	3H	d (*J* = 6.5 Hz)	6, 7, 8	H-7
14	18.02	0.90	3H	d (*J* = 6.7 Hz)	10, 11, 15	H-11
15	17.42	0.77	3H	d (*J* = 6.7 Hz)	10, 11, 14	H-11

386 **Table S6.** ^{1}H and ^{13}C NMR data of compound **3** ($CDCl_3$, 400 MHz and 101 MHz).

Position	^{13}C	^{1}H				
	δ(ppm)	δ(ppm)	Intensity	Multiplicity	HMBC correlation	COSY correlation
1	9.60	0.44	1H	dd (*J* = 9.9, 5.5 Hz)	2, 3, 6, 7, 10	H-1b, H-2
		0.06	1H	d (*J* = 5.7 Hz)	2, 3, 6, 7, 10	H-1a, H-2
2	24.33	0.85	1H	m		H-1
3	69.26					
4	30.39	1.17	1H	m		H-4b, H-5a
		1.07	1H	m	5, 10	H-4a
5	29.02	1.51	1H	m	3, 4, 6	H-4a
		1.18	1H	m		
6	34.41					
7	40.36	1.81	1H	m	2, 8	H-13
8	33.54	1.73	1H	m	7, 9, 10	H-8b
		1.15	1H	m		H-8a
9	32.17	1.66	1H	m	5, 8, 10, 11	H-9a
		1.13	1H	m		H-9b
10	43.33					
11	30.2	1.52	1H	m	5, 9, 10, 14, 15	H-14, H-15
12	29.6	1.24	3H	s	2, 3, 4	
13	14.29	0.60	3H	d (*J* = 6.4 Hz)	6, 7, 8	H-7
14	17.71	0.88	3H	d (*J* = 6.7 Hz))	10, 11, 15	H-11
15	17.36	0.77	3H	d (*J* = 6.6 Hz)	10, 11, 14	H-11

Table S7. ^{1}H and ^{13}C NMR data of compound **8** ($CDCl_3$, 400 MHz and 101 MHz).

Position	^{13}C	^{1}H				
	δ(ppm)	δ(ppm)	Intensity	Multiplicity	HMBC correlation	COSY correlation
1	33.18	1.86	1H	m	2, 3	H-2
		1.74	1H	m		H-2
2	120.6	5.34	1H	m		H-1a, H-1b
3	133.77					
4	28.07	2.01	1H	m		H-4b, H-5
		1.93	1H	m		H-4a, H-5
5	25.92	1.62	2H	m	1, 3, 4, 6, 7	H-4
6	49.75					
7	39.85	2.0	1H	m		H-8a, H-13
8	37.67	2.41	1H	ddt (*J* = 15.8, 6.7, 1.7 Hz)	9, 10, 13	H-7, H-8b, H-9
		1.71	1H	dt (*J* = 15.8, 2.8 Hz)	6, 7, 9, 10, 13	H-8a, H-9
9	119.49	5.32	1H	m	6, 7, 8	H-8a, H-8b
10	157.29					
11	26.18	2.17	1H	m	9, 10, 14, 15	H-14, H-15
12	23.52	1.66	3H	brs	2, 3, 4	
13	16.19	0.87	3H	d (*J* = 6.9 Hz)	6, 7, 8	H-13
14	24.19	1.02	3H	d (*J* = 7.2 Hz)	10, 11, 15	H-11
15	24.34	1.04	3H	d (*J* = 7.2 Hz)	10, 11, 14	H-11

389 **Table S8.** ^{13}C NMR data of ^{13}C-labeled compound **1** ($CDCl_3$, 101 MHz).

Position	δ(ppm)	Enrichment	Isotope shift (ppm)		
1	25.11	*		-0.11	
2	121.98				
3	138.39	*		-0.09	
4	29.06				
5	38.29	*		None	
6	137.93				
7	130.74	*		-0.08	
8	36.96				
9	28.13	*		None	
10	57.72				
11	33.34	*	-0.07	-0.15	-0.25
12	26.88				
13	13.71				
14	17.21				
15	17.96				

390

391 **Table S9.** ^{13}C NMR data of ^{13}C-labeled compound **8** ($CDCl_3$, 101 MHz).

Position	δ(ppm)	Enrichment	Isotope shift (ppm)	
1	33.18	*	-0.13	
2	120.6			
3	133.77	*	-0.08	
4	28.07			
5	25.92	*	None	
6	49.75			
7	39.85	*	-0.18	-0.27
8	37.67			
9	119.49	*	None	
10	157.29			
11	26.18	*	-0.14	-0.22
12	23.52			
13	16.19			
14	24.19			
15	24.34			

392

Coordinates and detailed data for quantum chemical calculations of compound 1.

Energy minimization of two conformations of **1** (**1a** and **1b**)

E(B3LYP-Aug-CC-pVDZ) = -586.08767

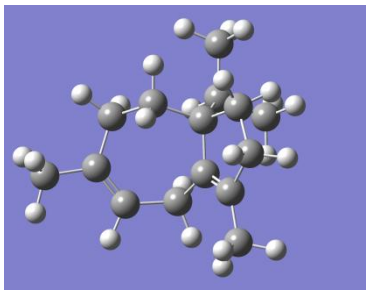

Standard orientation:

Center Number	Atomic Number	Atomic Type	Coordinates (Angstroms) X	Y	Z
1	6	0	0.715410	-0.456567	-0.350590
2	6	0	0.302078	0.844305	0.343414
3	6	0	-2.171125	0.706989	0.889280
4	6	0	0.716214	3.368861	0.186909
5	6	0	1.686957	-2.832758	0.000519
6	6	0	2.291002	-1.007483	1.628828
7	6	0	-4.071908	-0.278131	-0.365960
8	6	0	1.207855	-1.535472	0.673196
9	6	0	-0.474079	-0.985389	-1.202483
10	6	0	-2.627236	-0.253609	0.070152
11	6	0	-0.753661	0.848448	1.420864
12	6	0	0.903592	1.926844	-0.181224
13	6	0	1.859811	0.013354	-1.308054
14	6	0	1.824941	1.559178	-1.321804
15	6	0	-1.766892	-1.388854	-0.464433
16	1	0	-2.879276	1.470108	1.221720
17	1	0	0.034077	3.507567	1.033832
18	1	0	1.680384	3.835783	0.444544
19	1	0	0.311611	3.939279	-0.665083
20	1	0	0.891181	-3.329058	-0.568561
21	1	0	2.525850	-2.645319	-0.684837

22	1	0	2.037423	-3.545872	0.759953
23	1	0	2.519701	-1.763591	2.392705
24	1	0	3.229335	-0.783357	1.102308
25	1	0	1.972917	-0.092274	2.142799
26	1	0	-4.554257	-1.224173	-0.069900
27	1	0	-4.644912	0.551000	0.068087
28	1	0	-4.151793	-0.218307	-1.463753
29	1	0	0.345079	-1.802060	1.300762
30	1	0	-0.128145	-1.852991	-1.781710
31	1	0	-0.725047	-0.207936	-1.939460
32	1	0	-0.688941	1.781205	1.994068
33	1	0	-0.552727	0.041953	2.145543
34	1	0	1.735464	-0.410815	-2.312619
35	1	0	2.833623	-0.332271	-0.943802
36	1	0	2.826575	2.001872	-1.200740
37	1	0	1.432128	1.959150	-2.272494
38	1	0	-1.532563	-2.086531	0.355825
39	1	0	-2.375427	-1.971653	-1.170864

E(B3LYP-Aug-CC-pVDZ) = -586.08988

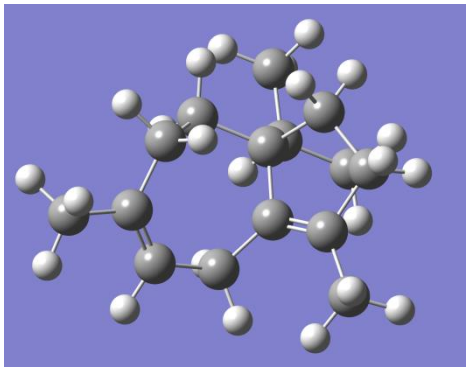

Standard orientation:

Center Number	Atomic Number	Atomic Type	Coordinates (Angstroms) X	Y	Z
1	6	0	-0.734267	-0.507604	0.237073
2	6	0	-0.114903	0.743956	-0.384314
3	6	0	2.249775	0.203403	-1.151359
4	6	0	-0.114527	3.290063	-0.084815

459	5	6	0	-2.392071	-2.459546	-0.192911
460	6	6	0	-2.935363	-0.182484	-1.107567
461	7	6	0	4.108884	-0.738384	0.189821
462	8	6	0	-1.798685	-1.143811	-0.725629
463	9	6	0	0.366649	-1.560768	0.538059
464	10	6	0	2.643802	-0.463408	-0.054363
465	11	6	0	0.844455	0.626998	-1.538243
466	12	6	0	-0.496058	1.875566	0.234921
467	13	6	0	-1.367894	0.055100	1.548538
468	14	6	0	-1.443964	1.588983	1.379422
469	15	6	0	1.713512	-0.996950	1.024949
470	16	1	0	3.024436	0.504384	-1.862669
471	17	1	0	0.552508	3.365367	-0.951306
472	18	1	0	-1.009410	3.900518	-0.287547
473	19	1	0	0.394309	3.759131	0.772654
474	20	1	0	-1.629934	-3.231487	-0.033764
475	21	1	0	-2.923883	-2.306536	0.757420
476	22	1	0	-3.119977	-2.862001	-0.911561
477	23	1	0	-3.580727	-0.644609	-1.867338
478	24	1	0	-3.571707	0.053213	-0.242720
479	25	1	0	-2.554042	0.760324	-1.517971
480	26	1	0	4.303137	-1.822111	0.238427
481	27	1	0	4.743802	-0.307383	-0.594556
482	28	1	0	4.428440	-0.320512	1.158649
483	29	1	0	-1.257332	-1.390848	-1.653666
484	30	1	0	0.555047	-2.163439	-0.363273
485	31	1	0	-0.014661	-2.257211	1.297937
486	32	1	0	0.917752	1.591370	-2.060176
487	33	1	0	0.445845	-0.074972	-2.291995
488	34	1	0	-0.718668	-0.187764	2.400225
489	35	1	0	-2.344329	-0.394793	1.764855
490	36	1	0	-2.462702	1.935170	1.135559
491	37	1	0	-1.151467	2.126559	2.295183
492	38	1	0	2.247278	-1.803543	1.549712
493	39	1	0	1.550215	-0.215508	1.786445
494	----------					